DEMOCRATIC AND POPULAR REPUBLIC OF ALGERIA

MINISTRY OF HIGHER EDUCATION AND SCIENTIFIC RESEARCH

20 AUGUST 1955- SKIKDA UNIVERSITY

FACULTY OF TECHNOLOGY

DEPARTMENT OF PROCESS ENGINEERING

Thesis

In view of obtaining the diploma of

Master

Field: Process Engineering

Speciality: Chemical Engineering

Removal of Malachite green from aqueous solution using HDPE-Clay composites

Submitted on 25/06/2023

Realized by:

TEBBAL Ahmed Rami

GUETTARI Ines

BOULHOUT Zaineb

Supervisor:

Dr. Bekouche Karima

Co-advisor:

Mr. Boudagha Seif El Islame

Academic year 2022/2023

الملخص

تعتبر التحسينات العديدة في خصائص المركبات النانوية المونتموريلونيت البوليمرية أمرًا مهمًا جدًا في البحوث والتطبيقات الصديقة للبيئة. في هذه الدراسة، تم استخدام تقنية الدمج بالانصهار لإعداد أفلام المركبات النانوية بناءً على البولي إيثيلين ذو الكثافة العالية والمونتموريلونيت (البنتونيت والمونتموريلونيت المعالج وصوديوم المونتموريلونيت). في البداية، تم الحصول على صوديوم المونتموريلونيت المعالج عن طريق تقنية تبادل الكاتيون للمونتموريلونيت المنقى، ثم تم إنتاج أفلام المركبات النانوية بنسبة تحميل المونتموريلونيت 4% وزنًا. تم توصيف المركبات النانوية المحضرة بواسطة مؤشر تدفق الانصهار، الكثافة، المجهرية البصرية والطيفية بالأشعة تحت الحمراء بتحويل فورييه. بالإضافة إلى ذلك، تم تقييم كفاءة المركبات النانوية المونتموريلونيت في امتصاص المالاكيت الأخضر باستخدام التحليل الطيفي. تم تحليل بيانات الامتصاص باستخدام نماذج ايزوثيرمبة وحركية مختلفة لفهم آلية الامتزاز. تشير النتائج التجريبية المستنتجة في هذا العمل إلى أن صوديوم المونتموريلونيت يتمتع بأداء جيد للامتزاز. نموذج الايزوثيرم لانجمير يصف سلوك الامتزاز بشكل أفضل، مشيرًا إلى امتزاز طبقة واحدة على سطح متجانس. أظهرت الدراسات الحركية أن عملية الامتزاز تتبع نموذج الكينتيك من الرتبة الثانية، مشيرة إلى أن الامتزاز الكيميائي هو الآلية السائدة.

الكلمات المفتاحية: المركب النانوي، فيلم، مونتموريلونيت، بولي ايثيلان، الامتزاز، المالاكيت الأخضر

ABSTRACT

The numerous enhancements in the properties of polymer montmorillonite nanocomposites make them very significant in research and eco-friendly applications. In this study, melt blending technique was used to elaborate nanocomposites films based on high density polyethylene (HDPE) and montmorillonites (bentonite, purified-montmorillonite and Na-montmorillonite). Initially, virgin Na-MMT was obtained by cation exchange technique of purified montmorillonite, and then the nanocomposites films were produced with a montmorillonite loading rate of 4%. the prepared nanocomposites were characterized by melt flow index, density, optical microscopy and Fourier transform infrared spectroscopy. In addition, the efficiency of HDPE/MMT's nanocomposites in malachite green adsorption was assessed spectroscopically. The adsorption data were analysed using different isotherm and kinetic models to educate the adsorption mechanism. The experimental results obtained in this present work indicate that the HDPE/Na-MMT has good adsorption performance. The Langmuir isotherm model described better the adsorption behaviour suggesting monolayer adsorption onto homogeneous surface. Kinetic studies revealed that the adsorption process followed pseudo-second-order model, indicating chemisorption as the governing mechanism.

Keywords: Nanocomposites, Film, Montmorillonite, HDPE, Adsorption, Malachite green.

RÉSUMÉ

Les nombreuses améliorations des propriétés des nanocomposites polymères montmorillonite les rendent très significatifs dans la recherche et les applications respectueuses de l'environnement. Dans cette étude, la technique de mélange en fusion a été utilisée pour élaborer des films nanocomposites à base de polyéthylène haute densité (HDPE) et de montmorillonites (bentonite, montmorillonite purifiée et Na-montmorillonite). Initialement, du Na-MMT vierge a été obtenu par la technique d'échange cationique de la montmorillonite purifiée, puis les films nanocomposites ont été produits avec un taux de charge en montmorillonite de 4 % en poids. Les nanocomposites préparés ont été caractérisés par l'indice de fluidité à chaud, la densité, la microscopie optique et la spectroscopie infrarouge à transformée de Fourier. De plus, l'efficacité des nanocomposites HDPE/MMT's dans l'adsorption du vert de malachite a été évaluée spectroscopiquement. Les données d'adsorption ont été analysées à l'aide de différents modèles d'isothermes et de cinétiques pour comprendre le mécanisme d'adsorption. Les résultats expérimentaux obtenus dans cette étude indiquent que le HDPE/Na-MMT présente de bonnes performances d'adsorption. Le modèle d'isotherme de Langmuir décrit mieux le comportement d'adsorption, suggérant une adsorption en monocouche sur une surface homogène. Les études cinétiques ont révélé que le processus d'adsorption suivait le modèle de pseudo-deuxième ordre, indiquant que la chimisorption était le mécanisme dominant.

Mots clés : Nanocomposites, Film, Montmorillonite, PEHD, Adsorption, Vert de malachite.

Acknowledgement

First and foremost, we thank Allah the one and only who gave us the health, the courage, the strength to resist and the will to accomplish this work.

We deeply thank our supervisor; Dr. **K. Bekouche** for her advice encouragement, and continuous guidance throughout this thesis.

We specially thank our co-advisor Mr. **S. Boudagha** for his constant interest in this work, his advice and his help.

Big thank you goes to Dr. **S. Guendouz** for her help.

We are also grateful to the members of the jury, for their valuable feedback.

We thank all the engineers of the laboratory of Sonatrach and laboratory of university. We express our deepest gratitude to all of our families.

Lastly; we would like to thank all those, who have contributed in one way or another in the realization of this thesis.

Thank you to all.

Dedication

I would like to dedicate this work to my father and to my mother, for their love, their sacrifices, for teaching me and extending me the maximum potential they could offer, for raising me to be real, for believing in me and making me the man I am

I dedicate this work to my brother, to my sisters, for their help, their caring, their love and their support

To my dear friend "Ru." who has been by my side during my tough times.

Thanks

Ahmed Rami

Dedication

I dedicate this humble work to the two dearest people

To my dearest mother Mounira and to my dearest father Azzedine

For their love, their support, for the prayers of my mother

During my most difficult moments.

Good health and long life

I also dedicate this work to:

To my dear sister Nardjes

To my brothers Oussama and Ahmed.

I wish them a future full of joy, happiness, success and

And to all the members of my family

To all my grandparents who have given their love and generosity

To all the laboratory engineers

To all my friends

To my lovely dogs and cats

To my second family “I-Tech skikda club”

To all the class of 2022/2023 Chemical Engineering.

And to all those who are dear to me

With all my affection

Thank you.

Ines

Dedication

To the memory of my beloved grandparents and my father.

Zaineb

Table of Contents

CHAPTER II: POLYMER/CLAY NANOCOMPOSITES

PART B: EXPERIMENTAL STUDY

CHAPTER III: MATERIALS AND METHODS

CHAPTER IV: RESULTS AND DISCUSSION

LIST OF FIGURES

CHAPTER I: GENERALITY ABOUT DYES AND ADSORPTION

CHAPTER II: POLYMER/CLAY NANOCOMPOSITES

CHAPTER III: MATERIALS AND METHODS

CHAPTER IV: RESULTS AND DISCUSSION

LIST OF TABLES

CHAPTER I: GENERALITY ABOUT DYES AND ADSORPTION

CHAPTER II: POLYMER/CLAY NANOCOMPOSITES

CHAPTER III: MATERIALS AND METHODS

CHAPTER IV: RESULTS AND DISCUSSION

LIST OF ABBREVIATIONS

C.I: Color Index

DF : Diffusion coefficient

DS : Diffusion coefficient

I.U.P.A.C: International Union of Pure and Applied Chemistry

MMT: Montmorillonite

T: Temperature (°C)

t: Time (min)

V: Volume of adsorbate (L)

q: Adsorption capacity

qe: Equilibrium concentration in the solid phase- adsorbate (mg / g)

qt: Amount of dye adsorbed by one gram of solid at time t (mg/g)

qmax: The maximum adsorption capacity (mg / g)

1/n: Adsorption intensity

C_e: The concentration of the adsorbate at equilibrium (mg / L)

C_0: Initial concentration (mg. L^{-1})

K_L: The Langmuir constant (min^{-1})

Kc: The equilibrium constant (qe / Ce)

K_T: The equilibrium binding constant ($L.g^{-1}$)

M: Molar mass of the adsorbent (g)

MG: Malachite green

R_L: Coefficient indicating the type of isotherm

KF and **n:** Coefficients characteristic of the adsorbate-adsorbent couple and of the experimental conditions

k_1: Rate constant of the pseudo-first order kinetic model (min^{-1})

k_2: The rate constant of the pseudo second order kinetic model ($g.mg^{-1}. min^{-1}$)

MFI: Melt Flow Index

HDPE: High density polyethylene

FTIR: Fourier-transform infrared spectroscopy

PNMs: Polymeric nanostructured materials

PLS: polymer/layered silicate

DP: Degree of polymerization

PCNs: polymer-clay nanocomposites

polyDADMAC: polydiallyldimethylammonium chloride

COD: chemical oxygen demand

ʎ: wavelength

GENERAL INTRODUCTION

General Introduction

Malachite green is widely used in aquaculture as a parasiticide and in food, health, textile and other industries for one or the other purposes. It controls fungal attacks, protozoan infections and some other diseases caused by helminths on a wide variety of fish and other aquatic organisms. However, the dye has generated much concern regarding its use, due to its reported toxic effects. Though the use of this dye has been banned in several countries it is still being used in many parts of the world due to its low-cost, ready availability and efficacy and to lack of a proper alternative **[1]**.

There are many processes available for dyes treatment: chemical oxidation, flotation, adsorption, electrolysis, chemical coagulation, photo catalysis and biodegradation. Among all these, adsorption has been found to be an efficient method for the removal of dyes from aqueous solutions because it produces high quality treated effluent and also allows kinetic and equilibrium measurements without any highly sophisticated instruments, many adsorbents are used in adsorption including activated carbon, silicia gels, clays and nanocomposites. One of the common composites is polymer/clay nanocomposites, which is eco-friendly, low-cost and effective **[2]**.

The objective of this study is to develop a nanocomposite films based on High density polyethylene polymer and montmorillonite and explore their potential application for malachite green adsorption. The analysis and characterization of the adsorbent will be conducted. Furthermore, the adsorption performance of HDPE/MMT nanocomposites will be assessed through batch adsorption experiments, with different parameters such as initial concentration, adsorbent weight, contact time, pH, temperature, etc.

Overall, this thesis will demonstrate the potential of HDPE/MMT nanocomposites as efficient and eco-friendly materials for colorant adsorption applications, such as water treatment. The insights that could be gained from this study can help to optimize the design and performance of nanocomposite films for specific colorant removal or recovery processes.

This thesis is organized in four chapters divided into two main parts, the first includes the theoretical side of the work, and the other the practical side;

Chapter I: This chapter covers two major topics. Firstly, we conducted a literature review on dyes and colorants, focusing on their classification, toxicity, and treatment methods. Secondly, we provided a general overview of adsorption phenomena, discussing various adsorption isotherm models and the key parameters influencing this phenomenon.

Chapter II: The chapter presents an overview of polymer/clay nanocomposites, an emerging class of materials that combine the advantages of polymers and clay nanoparticles, polymer and clay were examined separately, to gain a deeper understanding of their properties and behaviour within the nanocomposite system.

Chapter III: In this chapter we presented materials and methods used.

Chapter IV: In the last chapter we discussed our results concerning the elimination of malachite green using HDPE/MMT nanocomposites adsorbents.

Finally, a conclusion that summarizes the found results.

PART A:

BIBLIOGRAPHIC STUDY

CHAPTER I:

GENERALITY ABOUT DYES AND ADSORPTION

1. General information about dyes

1.1. History

The evolution of the dye industry was closely linked to the discovery of mauvéine (aniline, basic dye) by William Henry Perkin in 1856 and fuchsine by Verguin in 1858. Today there are more than 10,000 dyes, such a large number that a classification system was necessary and the Society of Dyers and Colourists has developed the English Dyes Index. (UK) and by the "American Association of textile chemists and colourists" noted (colour Index C.I.), which describes the essential characteristics of each dye such as: their chemical formula, their colour and shade, their coded resistance to light, solvents, heat, different chemical agents, as well as a description of the main areas of use **[3]**.

Dyes are colour chemical compounds, natural or synthetic, which can be fixed on a substrate and give it its colouring. The treatment which leads to this result is called according to the case: dyeing, printing, painting, coating, or coloration in the mass. The fixing of the dye takes place by adsorption, creation of chemical bonds or by simple adhesion in the substrate **[4].**

A dye has groups, called chromophores, which confer the color and auxochrome groups which allow its fixing. The usual chromophores and auxochromes are summarized in the table below:

Table I. 1: Main chromophore and auxochrome groups. **[4]**

Chromophore Groups	**Auxochrome Groups**
Azo (-N=N-)	Amino (-NH2)
Nitroso (-NO or -N-OH)	Methylamino (-NHCH3)
Carbonyl (=C=O)	Dimethylamino (-N(CH3)2)
Vinyl (-C=C-)	Hydroxyl (-HO)
Nitro (-NO_2 or =NO-OH)	Alkoxyl (-OR)
Sulphide (>C=S)	Electron donor groups

1.2. Classification of dyes

Dyes have a considerable variety of structures and are classified in several ways, by their chemical structure and by their application to the type of fiber. Dyes can also be classified according to their solubility. **[5]**

1.2.1. Chemical classification

The classification of dyes according to their chemical structure is based on the nature of the chromophore group **[6]**.

A. Azo dyes

The "azo" dyes are characterized by the azo functional group **(-N=N-)** uniting two identical or non-identical alkyl or aryl groups (symmetrical and dissymmetrical azo). These structures which are generally based on the azobenzene skeleton, are aromatic or pseudoaromatic systems linked by an azo chromophore group. **[6]**

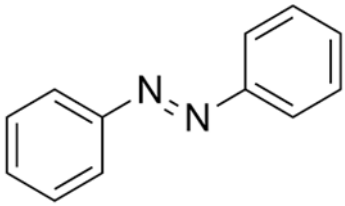

Figure I. 1: Azo dyes classification. **[6]**

B. Anthraquinonic dyes

From a commercial point of view, these dyes are the most important after the azo dyes. Their general formula derived from anthracene shows that the chromophore is a quinone ring to which hydroxyl or amine groups can be attached.

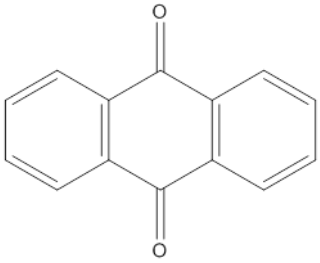

Figure I. 2: Anthraquinonic dyes classification. **[6]**

C. Indigoid dyes

They take their name from the Indigo from which they derive. Thus, the selenium, sulphur and oxygenated counterparts of Indigo Blue cause important hypsochrome effects with colours that can go from orange to turquoise.

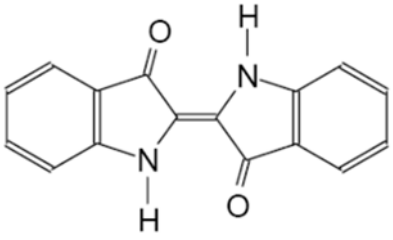

Figure I. 3: Indigoid dyes classification. **[6]**

D. Xanthene dyes

These dyes have an intense fluorescence. The best known compound is fluorescein. Little used as dye, their faculty of markers at the time of maritime accident or of tracers of flow for underground rivers is nevertheless well established.

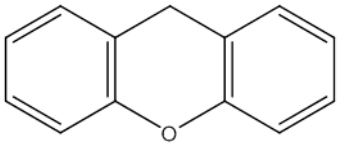

Figure I. 4: Xanthene dyes classifiction. **[6]**

E. Phthalocyanins dyes

They have a complex structure based on the central copper atom. The dyes of this group are obtained by reaction of dicyanobenzene in the presence of a metal halide (Cu, Ni, Co, Pt, etc.)

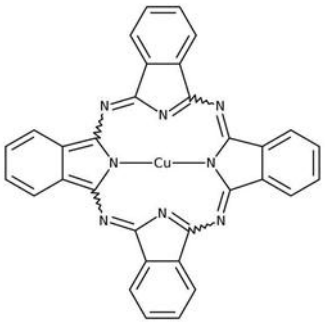

Figure I. 5: Phthalocyanins dyes classification. **[6]**

F. Nitrated and nitrosated dyes

These dyes are a relatively old class, very limited in number. They are still used today, because of their very moderate price linked to the simplicity of their molecular structure characterized by the presence of a nitro group (-NO2) in the ortho position of an electron-donor group (hydroxyl or amino groups).

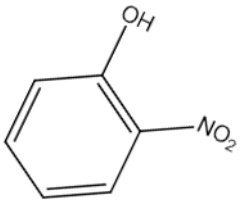

Figure I. 6: Nitrated and nitrosated dyes classification. **[6]**

G. Triphenylmethane dyes

Triphenylmethanes are methane derivatives in which the hydrogen atoms are replaced by substituted phenyl groups, at least one of which carries an oxygen or nitrogen atom in para position to the methane carbon. Triphenylmethane and its homologues constitute the basic hydrocarbons from which a whole series of colorants are derived.

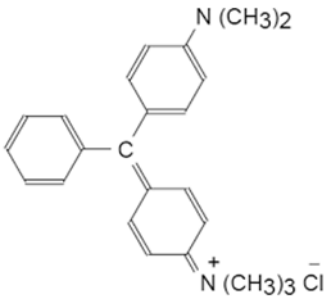

Figure I. 7: Triphenylmethan dyes classification. **[6]**

1.2.2. Source Classification

- Vegetable: indigo, madder, saffron, sorrel, cachou, turmeric, naprum, pastel, walnut gall, gaude, etc;
- Animal : cochineal, kernels, purple, etc ;
- Mineral: iron oxide, Prussian blue, graphite, etc **[7].**

1.2.3. Tectorial classification (method of application)

While the chemical classification is of interest to the dye manufacturer, the dyer prefers the classification by field of application **[5]**.

Thus, he is informed about the solubility of the dye in the dye bath, its affinity for the various fibers and the nature of the fixation. The strength of the binding varies according to whether the dye/substrate bond is ionic, hydrogen, Van der Waals or covalent. We distinguish different dye categories defined this time by the auxochromes **[3]**. The table I.2 shows the distinctive colours used in textile staining operations.

Table I. 2: Classification of dyes according to the application method. **[8]**

Dye class	Description
Acid	Water-soluble anionic compounds
Basic	Water-soluble, applied in weakly acidic dye baths; very bright dyes
Direct	Water-soluble, anionic compounds; can be applied directly to cellulosic without mordents (or metals like chromium and copper)
Disperse	Not water-soluble

Reactive	Water-soluble, anionic compounds; largest dye class
Sulphur	Organic compounds containing sulphur or sodium sulphide
Vat	Water-insoluble; oldest dyes; more chemically complex

1.3. Use and application of dyes

The major areas of application of dyes are **[9]**:

- In the textile industry of fur, leather (textile for clothing, decoration, building, transport, textile for medical use, etc.);
- In the plastics industry (pigments);
- In the building industry: paints (pigments), building materials, ceramics...;
- In the pharmaceutical industry (dyes);
- In the cosmetics industry (including hair colour);
- In the food industry (food colours and additives).

1.4. Toxicity and environmental impact

Dyes are compounds that are difficult to break down by microorganisms, and are toxic or harmful to humans and animals. Several research studies on the toxic effects of dyes on human health have been advanced.

Indeed, researchers have shown that amino dyes irritate the skin. Eczema and ulceration have been observed in factory workers manufacturing dyes of the triphenylmethane series **[10]**.

Allergic reactions, sometimes asthma and especially eczematous dermatitis have been observed with various amine azo dyes, anthraquinone dyes, as well as with some dyes of the naphthalene group. Synthetic amine dyes carry carcinogenic and urinary tumour risks, in particular benign and malignant tutors of the bladder **[11]**.

In aquatic environments, dye-laden textile industry waste in rivers can greatly affect animals, plants and microorganisms living in these waters. In addition, the biological degradation of dyes is very low, due to their molecular weight and their complex structures, give these complexes a toxic character that can be high or low **[12]**.

1.5. Treatment methods for dye-laden waters

Stringent requirements for the treatment of effluents have led to the search for less expensive methods to reduce their quantities **[13]**. A wide variety of thermal, physical, chemical and biological techniques are used in the treatment of textile effluents. The different processes allowing the elimination of dyes are described below.

A. Chemical:

- Chemical oxidation
- Precipitation
- Coagulation / Flocculation

B. Physic-chemical:

- Filtration
- Extraction
- Adsorption

C. Biological:

- Aerobic treatment
- Anaerobic treatment

2. Adsorption phenomena

2.1. Definition

Adsorption is a process that occurs when a gas or liquid solute accumulates on the surface of a solid or a liquid (adsorbent), forming a molecular or atomic film (the adsorbate). Adsorption is operative in most natural physical, biological, and chemical systems, and is widely used in industrial applications such as activated charcoal, synthetic resins and water purification. Among these methods, adsorption is currently considered very suitable for wastewater treatment because of its simplicity and cost effectiveness. Adsorption is commonly used technique for the removal of metal ions from various industrial effluents **[14]**.

2.2. Types of adsorption

2.2.1. Chemical adsorption (chemisorption)

It involves one or more covalent or ionic chemical bonds between the adsorbate and the adsorbent. Chemisorption is generally irreversible since it produces a monolayer. The heat of adsorption, relatively high, is between 20 and 200 Kcal/mol, the distance between the surface and the adsorbed molecule is shorter than in the case of physic-sorption **[15]**.

2.2.2. Physical adsorption (physisorption)

Physical adsorption is a reversible phenomenon that results from intermolecular forces of attraction between the molecules of the solid and those of the adsorbed substance (Van der Waals forces) **[15]**.

The difference between chemical adsorption and physical adsorption is shown in the table below:

Table I. 3: Main differences between the two types of adsorption. **[15]**

Comparisons criterions	Physical adsorption	Chemical adsorption
Nature of the interactions	Van Der Waal (weak bonds)	Chemical bonds
Heat of adsorption |Δ Hads|	<40 kJ/mol	>40 kJ/mol
Activation of the process	Process not activated	Process activated
Kinetics of the process	Spontaneous	Appreciative
Reversibility	Completely reversible	Often irreversible
Specificity	Non-specific	Specific
Equilibrium distance Mol-Surface	4 à 6 Å	<3Å
Number of adsorbed layers	Mono- or poly-molecular	Monomolecular
Temperature of the process	Low T°	High T°

2.3. Kinetics of adsorption

Adsorption kinetics describes the decrease in the concentration of the adsorbate in the solution as a function of contact time **[16].**

Knowledge of adsorption kinetics is of considerable practical interest in the optimal implementation of an adsorbent and in knowing which factors to optimize to make or improve an adsorbent leading to the fastest possible kinetics **[17]**.

The rate of adsorption of a solute from a solution depends on many factors, including the nature of the adsorbent, the adsorbate, as well as the agitation rate of the medium.

The literature provides several models that examine the mechanism(s) that control the adsorption process. Among these models, we distinguish the pseudo-first order model, the pseudo-second order model and the intra-particle diffusion model **[18]**.

2.3.1. Modelling of adsorption kinetics

The study of the adsorption kinetics gives information about the adsorption mechanism and the transfer mode of the adsorbates from the liquid phase to the solid phase. Indeed, several kinetic models have been developed to describe the adsorption kinetics. Among these models we quote below the most used models in the literature **[18]**.

2.3.1.1. Pseudo-first-order model

Lagergren (1898) proposed a pseudo first order kinetic model expressed by the following relation **[19]**:

$$\frac{dq_e}{dt} = k_1(q_e - q_t) \qquad \textbf{(I.1)}$$

With $\mathbf{k_1}$ the rate constant for pseudo first order kinetics [min^{-1}], $\mathbf{q_t}$ and $\mathbf{q_e}$ the adsorption capacities at time t [mg adsorbate / g adsorbent] and at equilibrium [mg of adsorbate / g of adsorbent], respectively **[19]**.

Integration of equation **(I.1)** gives:

$$\ln(q_e - q_t) = \ln q_e - k_1 t \qquad \textbf{(I.2)}$$

2.3.1.2. Pseudo-second-order model

An expression also very often used is that of the pseudo-second order, this model suggests the existence of chemisorption, an exchange of electrons for example between the adsorbate molecule and the solid adsorbent; it is represented by the following formula:

$$\frac{dq_e}{dt} = k_2(q_e - q_t)^2 \qquad \textbf{(I.3)}$$

With $\mathbf{k_2}$ the rate constant for second order kinetics [$g.mg^{-1}.min^{-1}$], q_t and q_e the adsorption capacities at time t [mg adsorbate /g adsorbent)] and at equilibrium [mg adsorbate/g adsorbent], respectively. Integration of equation **(I.3)** gives **[20]**:

$$\frac{t}{q_t} = \frac{1}{k_2 q_e^2} + \frac{1}{q_e} t \qquad \textbf{(I.4)}$$

2.3.1.3. Intra-articular dissemination model

Intra-articular diffusion is frequently the limiting step in many adsorption process. The possibility of intra-articular diffusion can be evidence using the theory-based model of Weber and Morris **[21]**.

$$q_e = k_d \sqrt{t} + c \qquad \textbf{(I.5)}$$

Where $\mathbf{K_d}$ is the intra-articular diffusion rate constant ($mg/g.min^{-1/2}$) that can be calculated as carrying the adsorbed amount as a function of $t^{1/2}$.

2.4. Adsorption mechanism

Adsorption occurs mainly in four stages. Figure.I.8 represents a material (adsorbent) with the different domains in which the organic or inorganic molecules which are likely to interact with the solid. **[22]**:

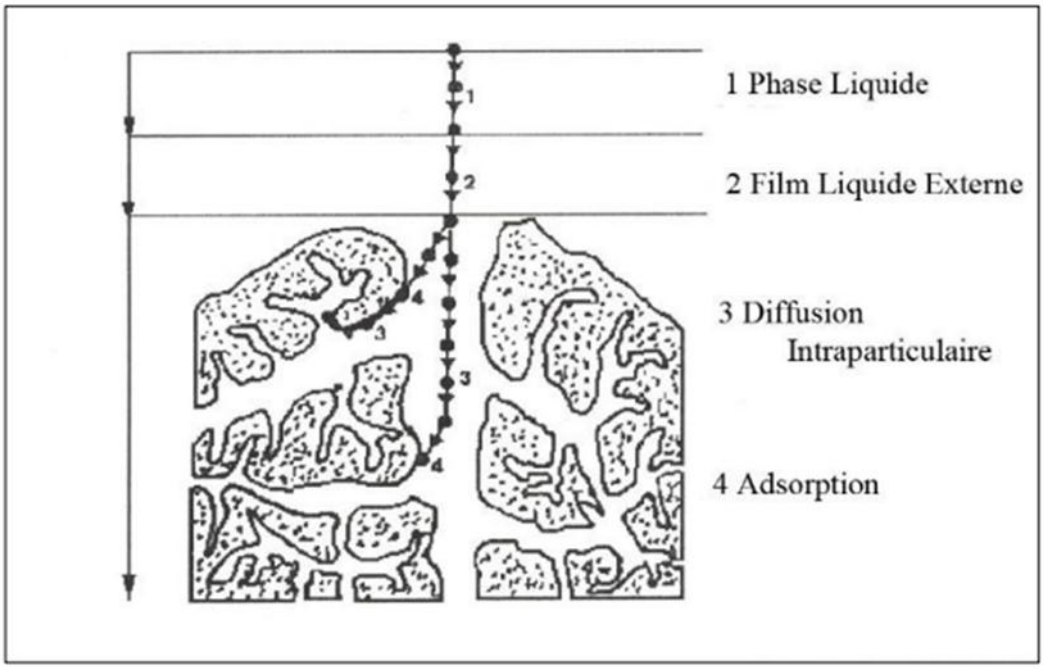

Figure I. 8: Different stages of transfer of a solute during its adsorption on a micro-porous material micro-porous material; after WEBER and SMITH. **[22]**

A. **First step (external diffusion):** transfer of solute molecules from the liquid phase external to the liquid phase bound to the solid particle (by diffusion and convection).
B. **Second step (internal diffusion):** transfer of the solute through the liquid film to the external surface of the adsorbent (characterized by the transfer coefficient K_f).
C. **Third step:** diffusion of adsorbate inside the particle of the adsorbent under the effect concentration gradient. The adsorbat molecule can diffuse from an adsorption site to an either in the Free State (after desorption) in the intraparticulate liquid phase (migration characterised by a diffusion coefficient DF), or in the adsorbed state, from an adsorption site to an adjacent site (surface migration characterized by a diffusion coefficient DS).
D. **Fourth step:** adsorption reaction in contact with the active sites, once adsorbed, the molecule is considered immobile **[22]**.

2.5. Application fields of adsorption

The many technical applications of adsorption are the result of three characteristics which differentiate it from other separation processes, namely **[23]**:

- Retention of very small particles, such as colloids;
- Retention of components at very low concentrations, such as impurities or metallic molecules and ions that give the product colours, odours, or unpleasant flavours or toxicity;
- The selectivity of adsorbent to certain components of the mixture.

Applications include the following **[23]**:

- The drying ;
- purification and deodorization of gases;
- Refining of petroleum products ;
- The contact catalysis ;
- Dehumidification and deodorization of air;
- Recovery of volatile solvents and alcohol in the process of fermentation;
- Discoloration of liquids ;
- Gas chromatography.

2.6. Adsorption isotherms

2.6.1. Adsorption isotherms classification

The adsorption isotherm represents the adsorbed quantities of solute as a function of its concentration in solution at a given temperature (Figure.I.9). The shape of the isotherm curve varies according to the adsorbate-adsorbent couple studied **[24]**.

Experimentally, there are four main classes named:

- **Class S (Sigmoid):** Indicates a vertical adsorption of polar mono-functional molecules, on a polar adsorbent and in a polar solvent;
- **Class L (Langmuir):** Indicates a flat adsorption of bi-functional molecules;
- **Class H (High affinity):** Does not start with zero but at a positive value, indicates a high affinity. Means that at low concentrations the adsorption is total;
- **Class C (Constant partition):** Increasing straight line, means that there is competition between the solvent and the solute to occupy the sites, with always the same partitioning (constant partitioning); concerns flexible molecules that can penetrate far into the pores to displace the solvent.

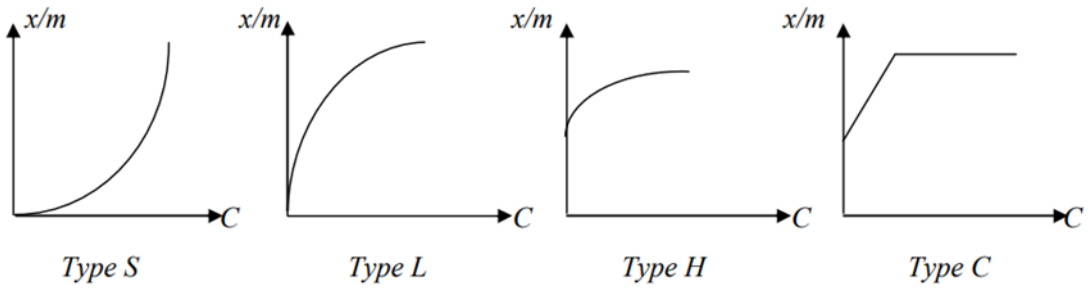

Figure I. 9 : Classification of isotherm form **[24].**

2.6.2. Modeling of adsorption isotherms

2.6.2.1. Langmuir model

The linearized form of Langmuir model can be written as

$$\frac{C_e}{Q_e} = \frac{1}{q_{max} K_L} + \frac{1}{q_{max}} C_e \qquad \textbf{(I.6)}$$

Here **Ce** and $\mathbf{q_e}$ represent the equilibrium concentration (mg/L) and adsorption capacity respectively.

$\mathbf{K_L}$ and $\mathbf{R_L}$ are characteristic Langmuir parameters which is termed as Langmuir adsorption constant and separation factor respectively. R_L is expressed as

$$R_L = \frac{1}{1 + K_L C_0} \qquad \textbf{(I.7)}$$

Here, $\mathbf{C_0}$ is initial dye concentration which is expressed in mg/L.

The value of $\mathbf{R_L}$ is related to feasibility or favorability of the adsorption process.

The relationship between R_L and the favorability of the adsorption is as follows:

- $\mathbf{R_L}$ value in the range of 0 and 1 implies favourable adsorption
- $\mathbf{R_L > 1}$ indicates unfavourable while
- $\mathbf{R_L = 0}$ and $\mathbf{R_L = 1}$ indicates reversible and linear adsorption respectively **[25]**.

2.6.2.2. Freundlich model

The Freundlich isotherm is represented as follow:

$$\ln(q_e) = \ln K_f + \left(\frac{1}{n}\right) * \ln(C_e) \qquad \textbf{(I.8)}$$

Where $\mathbf{C_e}$ and $\mathbf{q_e}$ are equilibrium adsorption concentration and equilibrium adsorption capacity respectively.

$\mathbf{K_F}$ and **n** are Freundlich constants and are related to adsorption capacity and adsorption intensity respectively.

- The plot of ln (q_e) versus ln (C_e) gives a straight line with intercept K_F and 1/n as slope;
- The value of 1/n is related to the favourability of the adsorption process;
- The value of 1/n in the range of 0 and 1 is considered as favourable adsorption **[26]**.

2.6.2.3. Temkin model

The Temkin model is based on the assumption that some indirect sorbate/adsorbate interactions are responsible of the linear decrease of the adsorption heat of all the molecules in the layer with coverage **[27]**.

The Temkin model is described by the following Eq **(I.9)**:

$$q_e = \frac{RT}{b}\ln(K_T C_e) \qquad \textbf{(I.9)}$$

Where $\mathbf{k_T}$ ($L.g^{-1}$) is the equilibrium binding constant, **b** ($J.mol^{-1}$) is related to heat of adsorption, **R** is the universal gas constant (8.314 $J.mol^{-1}.K^{-1}$) and **T (K)** is the absolute temperature.

2.7. Factors influencing adsorption equilibrium

The adsorption balance between an adsorbent and an adsorbate depends on many factors, the main ones of which are described below:

- **The specific surface:** is an essential measure of the sorption capacity of the adsorbent. It means the accessible area reported to the unit of adsorbent weight. A specific area is all the greater, if the adsorbent is more divided. Porosity: Porosity is related to the distribution of pore size. It reflects the inert structure of micro-porous adsorbents **[28]**;
- **Nature of the adsorbent:** Any solid is a potential adsorbent **[29]**;
- **Polarity:** A polar solute will have more affinity for the solvent or for the adsorbent, depending on which is more polar **[29]**;

- **pH:** pH sometimes has a significant effect on the adsorption characteristics. In most cases, the best results are obtained at the lowest pH, this property applies particularly to the adsorption of acidic substances **[30]**;
- **Temperature:** Adsorption is exothermic from which the results are better at relatively low temperatures **[31]**.

2.8. Adsorbents

The table below summarises the main industrial adsorbents, their selection criteria and their physical properties **[32]**:

Table I. 4: Main industrial adsorbents **[32]**.

Main industrial adsorbents	Selection criteria for industrial adsorbents	Physical properties of adsorbents
- Clays and bleaching earth - Silica gels - Activated alumina and bauxite - Molecular sieves - Activated carbon Animal black (obtained from the carbonization of bones)	- High adsorption capacity - High efficiency - High selectivity - Physical resistance - Chemical inertia - Ability to be easily regenerated - Low price	- Internal porosity - External void fraction ε corresponding to a bulk packing - Bulk density of the bulk layer - Density of the particle - True density - Specific pore area - Average pore radius - Theoretical adsorption capacity corresponding to the maximum amount of solute that can be adsorbed under the operating conditions per unit mass of fresh adsorbent

2.9. Advantages and disadvantages

A. Advantages of adsorption

- Wide use on a wide range of substances;
- Good reproducibility from laboratory to industrial scale;
- Possibility of multiple regeneration;
- Ease of implementation and operation **[33]**.

B. Disadvantages of adsorption

- Necessity of preliminary tests in laboratory;
- Risks of release (desorption);
- Not suitable for the treatment of highly charged effluents (saturation);
- Production of by-products after adsorption (pollution transfer) **[33]**.

CHAPTER II: POLYMER/CLAY NANOCOMPOSITES

Introduction

Many modern technologies use composite materials with properties that traditional materials cannot offer. Composite materials could be an effective solution to solve environmental, biodegradability and oil depletion problems. Over the past 20 years, materials and structures with geometric dimensions below 100 nm have earned increasing appeal in the scientific world and have stimulated the spirit of research on sometimes fanciful ideas for future applications. such as molecular manufacturing or space elevators as well as health, medical technology or food **[34, 35]**.

In this chapter, we will draw up state of the art knowledge on clay nanocomposites. First, a comprehensive description of clay and bentonite in terms of chemical structure and properties. Second, we will introduce the polymers in terms of structure, classification, and different synthesis techniques. We will end this chapter by discussing Polymer/clay Nanocomposites and methods of their preparation.

1. Clays

1.1. Definition

The term "clay" refers to a naturally occurring material composed primarily of fine-grained minerals, which is generally plastic at appropriate water contents and will harden with dried or fired. Although clay usually contains phyllosilicates, it may contain other materials that impart plasticity and harden when dried or fired. Associated phases in clay may include materials that do not impart plasticity and organic matter **[36]**. Additionally, the chief constituents of all clays are alumina and silica, the latter being always in excess of the former. These two oxides are, apparently, combined to form a hydro-alumino-silicate or alumino-silicic acid corresponding to the formula $H_4Al_2Si_2O_9$, but many clays contain a much larger proportion of silica than is required to form this compound, and other alumino-silicates also occur in them in varying proportions **[37]**.

1.2. Structure of clay minerals

Clay mineral is any of a group of important hydrous aluminum silicates with a layer (sheet-like) structure and very small particle size. They also may contain significant amounts of iron, alkali metals, or alkaline earths.

The development of microscopic and thermal procedures such as X-ray diffraction techniques enabled researchers to uncover that clays are composed of crystalline minerals **[38]**.

Essentially, clay minerals are composed of silica, alumina or magnesia or both, and water, but iron substitutes for aluminum and magnesium in varying degrees, and appreciable quantities of potassium, sodium, and calcium are frequently present as well. Some clay minerals may be expressed using ideal chemical formulas as the following: $2SiO_2 \cdot Al_2O_3 \cdot 2H_2O$ (kaolinite), $4SiO_2 \cdot Al_2O_3 \cdot H_2O$ (pyrophyllite), $Mg_3Si_4O_{10}(OH)_2$ (talc), and $3SiO_2 \cdot Al_2O_3 \cdot 5FeO \cdot 4H_2O$ (chamosite). The SiO_2 ratio in a formula is the key factor determining clay mineral types **[39]**.

Moreover, most clays in natural settings have a phyllosilicate or sheet structure. Such a structure implies that the ratio of particle dimensions is somewhat akin to that of a sheet of paper, that is to say, much larger and longer than thick **[38]**.

On this account, there exist two types of clay minerals and each has its atomic structure.

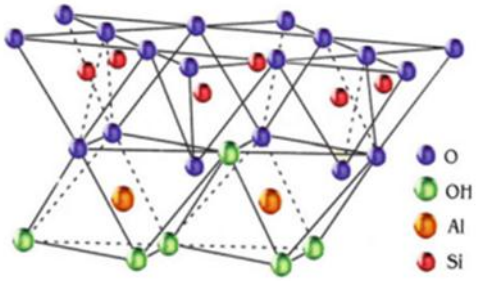

Figure II. 1: Clay structure **[40]**.

1.2.1. Tetrahedral sheet

The main dominating atom in the tetrahedral sheet is found in form of Si^{4+} cation. The basic building block of tetrahedral sheet is a unit of Si atom surrounded by four oxygen atoms known as silica tetrahedra as shown in Figure I.2. The tetrahedral sheet is formed by sharing of three oxygen of each tetrahedra with three nearest tetrahedra **[41]**. Al^{3+} frequently substitutes Si^{4+} and Fe^{3+} occasionally. The T/O (oxygen) ratio for layer silicates is T_2O_5 **[42]**. It is designated as T.

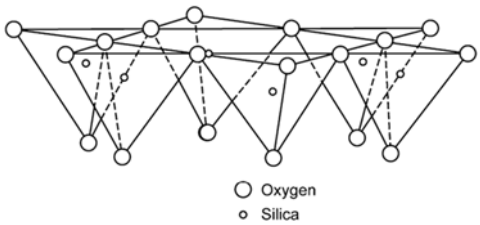

Figure II. 2 : Diagrammatic sketch of the tetrahedral sheet. **[42]**

1.2.2. Octahedral sheet

The main dominating atoms in octahedral sheets are Al^{3+} or Mg^{2+} surrounded by six oxygen atoms as demonstrated in Figure II.3. Often, hydroxyl group give rise to eight sided building block known as octahedron. Since, octahedral sheet are present in two forms: dioctahedral or trioctahedral sheet **[41]**. It is designated as O.

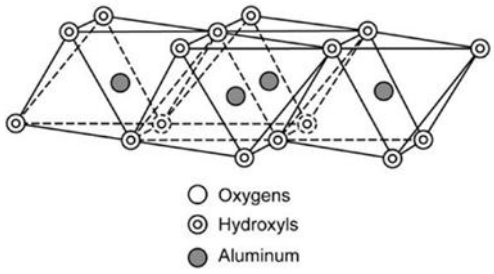

Figure II. 3: Diagrammatic sketch of the octahedral sheet. **[41]**

1.3. Properties of clay minerals

The special properties of clay minerals are due to the small particle size, the sheet structure and their variable charge.

1.3.1. Cation exchange capacity

The clays have the property to fix in an exchangeable way cations contained in the surrounding solutions. The cation exchange capacity (CEC) is defined by the number of exchangeable charges by a given mass of clay. It is expressed in milliequivalents per 100 g of clay (meq/100g). This characteristic depends on the nature of the clay (type of clay), its crystallographic characteristics, its cations and the pH of the medium. The cationic exchange capacity of a clay results from the iso-morphic substitution of aluminium atoms of the octahedral layer by Mg^{2+} and Fe^{3+} atoms. and Fe^{3+} atoms and of substitution of Si^{4+} by Al^{3+} in the tetrahedral layer inducing a deficit in charge of the sheet which is compensated by the presence of compensating cations There are different methods of measuring CEC. In general, one saturates natural clay with a solution containing an excess of cations, then an elemental analysis is carried out to evaluate the Elemental analysis to evaluate the quantity of cations exchanged between the clay and the solution. This measurement is generally done with NH^{4+} or Ba^{2+} cations. The determination by elemental microanalysis of the ions present in the clay substitution allows determining the CEC **[43]**.

1.3.2. Specific surface of clays

The specific surface is an essential property in the characterization of materials porous materials, it designates all the surfaces accessible to ionic particles, it is expressed in m^2 /g.

The fine size of the clay gives it a large surface area in relation to the size of the particles. Clays have a very large surface area combined with a very large contrast [**44]**. Distinguishing clay with three surfaces:

- The surfaces of the external planes forming the bases of the particles, these are the external surfaces;
- The cumulated surfaces of all the planes of the sheets, which limit the interfoliar spaces, called internal surfaces;
- The surfaces which mark laterally the limits of the sheets, they are the lateral surfaces.

The increase of the specific surface gives a higher swelling power and consequently a higher swelling potential **[43]**.

1.3.3. Swelling capacity

The degree of hydration varies from one clay family to another. Some clay minerals have the capacity to incorporate in their structure molecules of water. This water modifies the dimension of the layer by causing its swelling. These clays are called swelling clays. One distinguishes two types of swelling

- Water penetrates intramolecularly and organizes itself into monomolecular layers (inter-foliar swelling);
- Clay hydration, where water does not penetrate inside the clay particles. This phenomenon is reversible, as it can dry or swell again while maintaining its properties (inter-particle swelling).

there are minerals with adsorbed water but which do not have swelling properties (group of fibrous clays). Contrary to the interfoliar or intra particulate swelling, there is the interparticular swelling, that is to say that water does not penetrate inside the clay particles. This swelling has a limited extent, but affects all clays **[43]**.

1.3.4. Colloidality

This property is of great importance for the clay purification process. It is linked to the presence of negative charges on the surface of each clay grain. The colloidal character is translated by the covering of each clay grain by a double layer of water-soluble ions of opposite charges **[43]**.

1.4. Classification of clay minerals

Many different classifications of clay minerals have been suggested. A committee on the terminology of the Clay Minerals Group of the Mineralogy Society of Great Britain suggested that the crystalline clay minerals be divided into chain and layer structures and that the layer structures be divided into 2:1 (TOT) and 1:1 (TO) families, in addition to 2:1:1 TOTO **[45]**.

On the basis of the number and arrangement of tetrahedral (silica) and octahedral (alumina-magnesia) sheets contained in the crystal units or layers, silicate clays are classified into three different groups:

1.4.1. Type Minerals TO

Layered 1:1 minerals contain one tetrahedral and one octahedral sheet in their basic structural unit. Kaolinite is the most common mineral in this group. The sheets are held together by van der Waals bonds between the basic oxygens of the tetrahedral sheet and the hydroxyls of the octahedral sheet. The layers are held tightly together by hydrogen bonds, which restricts expansion and limits the reactive area to external surfaces. Isomorphic substitution for Si^{4+} and Al^{3+} in this mineral is negligible, due to the fact that the tetrahedral cation sites are usually occupied by Si^{4+} and the octahedral sites by all Al^{3+} or all Mg^{2+}. Soils dominated by minerals 1:1 exhibit a low capacity for adsorbing cations and have low fertility. Dioctahedral and trioctahedral types of silicate layer 1:1 exist as the serpentine group, with the general formula $Mg_3Si_2O_5(OH)_4$ **[46, 47]**.

1.4.2. Type Minerals TOT

Joining two tetrahedral sheets (one on each side) to an octahedral sheet results in a type of three-sheet mineral, called 2:1 and represented by groups of mica, smectite, and vermiculite. Its crystal structure consists of layers of two tetrahedral coordinated silicon atoms fused to an edge-shared octahedral sheet of aluminum or magnesium hydroxide. Adjacent layers of these minerals are bound together by van der Waals bonds. A silicon ion (Si^{4+}) is substituted for an aluminum ion (Al^{3+}) in every fourth tetrahedron. This results in an excess of one negative charge per formula. This negative charge is satisfied by potassium (K+) present at the interlayer sites between the layers 2:1 **[46, 47]**.

1.4.3. Type Minerals TOTO

This class of minerals exhibits a structure similar to that of a 2:1 layer, but with an interlayer of a gibbsite-like sheet, forming a 2:1:1 structural arrangement. The negative charge generated by the 2:1 layers balances the net charge created by isomorphic substitutions within

the interlayer hydroxide sheet. The typical formula for the interlayer is $(MgFeAl)(OH)^{6+}$. These minerals are non-expandable materials due to the inability to adsorb water in the interfacial space **[48]**.

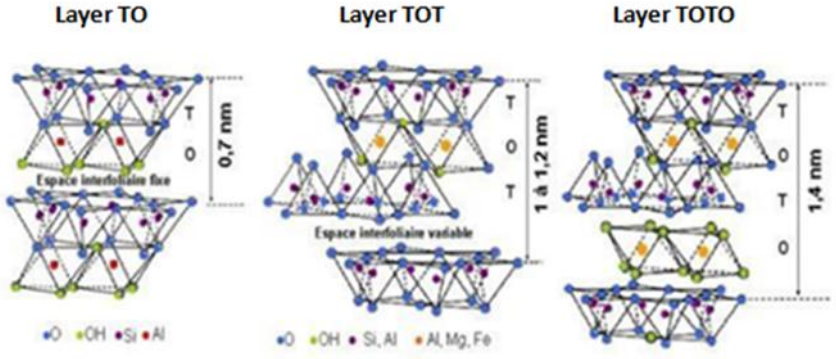

Figure II. 4: Schematic representation of clay sheet structures **[46]**.

1.5. Group of Clays

1.5.1. Kaolin

Kaolin group includes clay minerals like kaolinite, hallosite, nacrite and dickite, is a 1:1 type clay mineral. It is composed of one layer of silica and one layer of alumina, which is formed under acidic conditions through advanced weathering processes or hydrothermal changes of feldspars and other alluminosilicates. The chemical formula of kaolinite is $Al_2O_3.2SiO_2.2H_2O$ (39% Al_2O_3, 46.5% SiO_2 and 14.0% H_2O) and its structure possesses strong binding forces between the layers which resists expansion when wetted **[49]**.

The cation exchange capacity (CEC) of kaolinite is less than that of montmorillonite due to its low surface area and low isomorphous substitution that result from its high molecular stability and this contributes to its low plasticity, cohesion, shrinkage and swelling **[50]**.

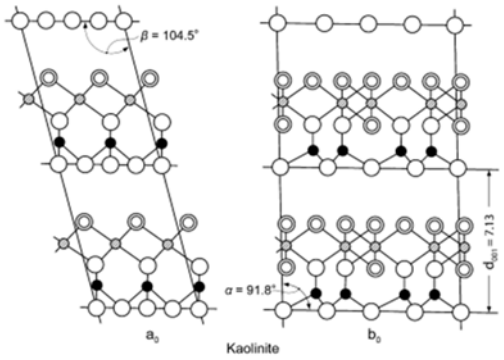

Figure II. 5: Schematic representation of the crystal structure of kaolinite **[51]**.

1.5.2. Illite

It is called clay micas Mica is a phyllosilicate mineral group that can be split or delaminated into thin sheets that are platy, flexible, clean, elastic, transparent to opaque, resilient, reflective, refractive, dielectric, chemically inert, insulating, light weight and hydrophilic **[44]**. Illite contains a higher percentage of water molecules than its host minerals, and it also contains a lower amount of potassium. The illite lattice is difficult to expand because water molecules have great difficulty in approaching the interlayer region **[47]**.

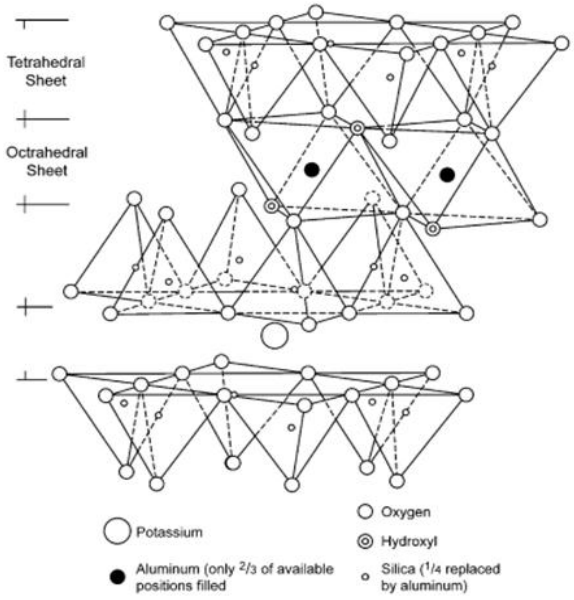

Figure II. 6: Diagrammatic sketch of the structure of illite **[51]**.

1.5.3. Vermiculite

Vermiculite is a hydrated magnesium aluminium-iron silicate which possesses 2:1 type of clay minerals. It has a layer charge of 0.9-0.6 per formula unit, and contains hydrated exchangeable cations primarily Ca, and Mg in the interlayer. The high charge per formula unit gives vermiculite a high cation exchange capacity and causes this clay type to have a high affinity of weakly hydrated cations such as K^+, NH^{4+} and Cs **[50]**.

1.5.4. Chlorites

Chlorites are hydrous aluminosilicates that are arranged in a 2:1 structure with an interlayer. They incorporate primarily Mg, Al and Fe cations and to a less extent Cr, Ni, Mn, V, Cu and Li cations in the octahedral sheet within the 2:1 layer and in the interlayer hydroxide sheet. They also exhibit a large substitution of Si by Al cations in the tetrahedral sheet. The colour of chlorites varies from white to almost black or brown with a tint of green where these optical properties are coupled to the chemical composition of chlorite **[49]**.

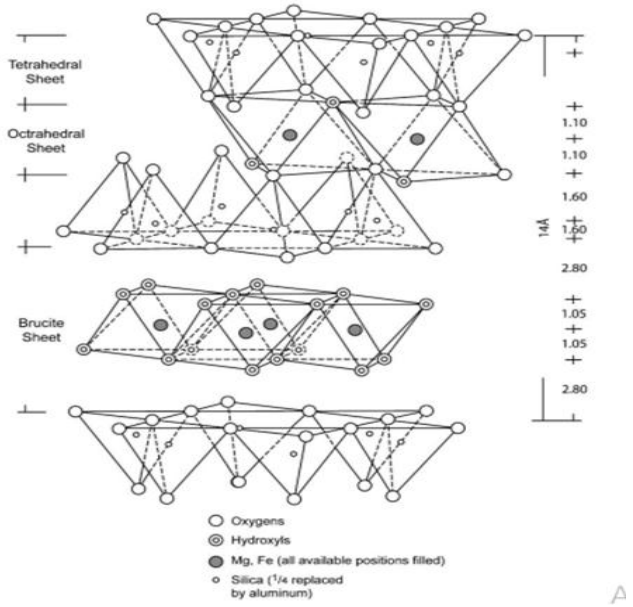

Figure II. 7 : Diagrammatic sketch of the structure of chlorite **[51]**.

1.5.5. Smectite

Smectite, which includes montmorrilonite, beidellite, nantronite, saponite and hectorite, are 2:1 layer clay minerals formed from the weathering of soils, rocks (mainly bentonite) or volcanic ash and belongs to a group of hydroxyl alumino-silicate. The variation of physical and chemical properties of bentonites within and between deposits is caused by differences in the degree of chemical substitution within the smectite structure, the nature of the exchangeable cations present, type and the amount of impurities present **[50]**.

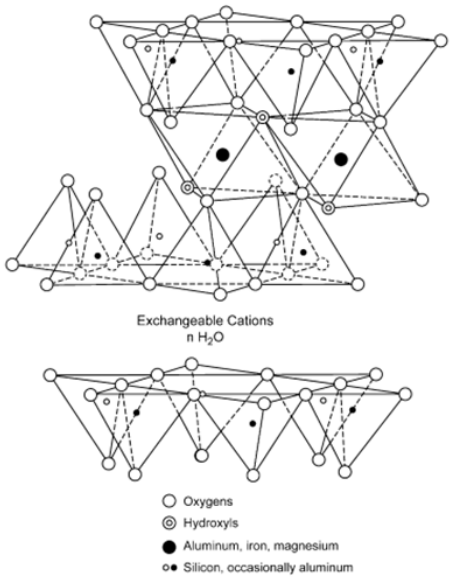

Figure II. 8: Diagrammatic sketch of the structure of smectites **[51]**.

1.5.6. Bentonite

The term bentonite designates a clay composed essentially of montmorillonite of the smectic group and which is characterized by a high swelling capacity (absorbency) after absorption of a liquid: water or an organic liquidSmectics are characterized by a sheet structure (reticular distance 14A°) made up of two tetrahedral and octahedral layers depending on the position of the oxygen or the hydroxyl (OH), the small cations (Si^{4+}, Al^{3+}, Fe^{3+}, Fe^{2+}, Mg^{2+}) lodge in the cavities of tetrahedra and octahedra.

Bentonites are hydrated alumina silicates belonging to the group of Montmorillonites with the formula:

Si_4 (Al (2-x) Rx) (O_{10}, H_2O) (Cex, nH_2O) or Si_4 (Al (2-x) Rx) (H_2O) n with:

- R = Mg, Fe, Mn, Zn, Ni
- Ce (exchangeable cations) = Ca, Na, Mg **[52]**.

1.5.6.1. Origin of bentonites

Bentonites are clays of volcanic origin, consisting mainly of montmorillonite; weathering and hydrothermal transformation of ash from glass-rich volcanic tuffs leads to the neoformation of clay minerals, which are part of the mainly from the smectite group. The clayey rocks thus formed bear the name bentonite, from the deposit near Fort Benton.It contains more than 75% montmorillonite; the latter was discovered for the first time in 1847 near Montmorillon, in the department of Vienne (France). Bentonite is a name for montmorillonite. The latter was discovered in clay deposits located near Montmorillon in Vienne, France. The bentonites discovered in 1888 contain at least 75% montmorillonite. In its natural raw form, bentonite is a soft rock having approximately the consistency of kaolin, i.e. friable, creamy to the touch; its color is white, gray or slightly tinged with yellow. It comes from devitrification of volcanic layers under the influence of alkaline reaction waters or acid. In addition to montmorillonite, this soil may contain other clay minerals (kaolinite, illite...) as well as impurities in the form of gypsum, carbonates, etc **[52]**.

1.5.6.2. Structure and composition of bentonites

Montmorillonite $(OH)_4$ Si8($Al_{10/3}$, $Mg_{2/3}$) O_{20}, nH_2O, **(**Figure II.9**)** is the main constituent of bentonite. It is a 2:1 phyllosilicate (smectite family) in which the negative charge of the layer is electrically balanced by an equal charge, exchangeable cations (Ca, Mg, H^+, K^+, NH and Na^+) located mainly between these layers silicates; these cations are not part of the structure and retain certain mobility **[53]**.

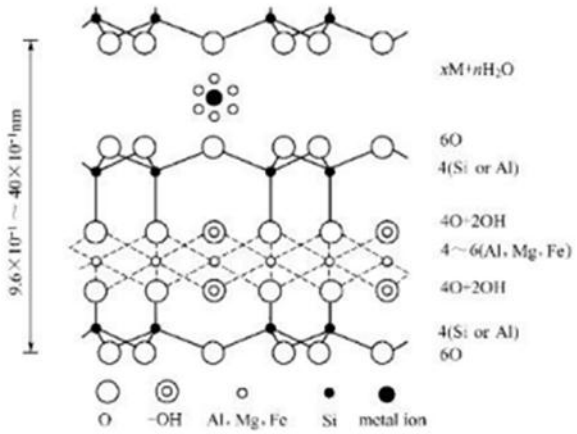

Figure II. 9: Schematic representation of the crystal structure of MMT **[52]**.

1.5.6.3. Use of bentonite

Bentonites are characterized by a high capacity of adsorption, ionic exchange and swelling, as well as by particular rheological properties (thixotropy). They have therefore applications in various fields (drilling, foundry, ceramics, paint, pharmaceuticals, etc.), foundry, ceramics, paint, pharmaceuticals, bleaching earth, etc.). Most of the bentonite exploited in the world is used as a binder for moulding sand, in the in the foundry industry and also to thicken drilling fluids. For many technical applications, raw bentonites must be subjected to a preparation adapted to the adapted to the requirements of their use (activation). For example, in the case of alkaline activation, calcium bentonites (the most common) are converted into sodium bentonites by treatment with soda ash, which are characterized in particular by a higher swelling capacity. Activation with acids such as hydrochloric acid increases the porosity by peripheral dissolution of the smectites. This results in a product with a high adsorption capacity.

They are used for operations of clarification or protein stabilization of musts and wines. Bentonites fix certain unstable proteins and thus allow their elimination. Bentonites are able to fix coloring matter **[54]**.

2. Polymers

2.1. History

The history of polymers dates back to the mid-19th century when scientists first discovered that natural polymers such as rubber and cellulose could be used for various applications **[55]**. The modern era of polymer science began in the early of 20th century, Leo Baekeland was the one who invented the first synthetic polymer (Bakelite), in 1907 **[56]**. However it was not until the 1920s and 1930s that synthetic polymers such as polystyrene and polyvinyl chloride were first developed **[57]**. Since then, the field of polymer science and

engineering has grown rapidly leading to the development of new materials with improved properties and performance; some of the most significant advances have come from the development of new synthesis methods, such as nanotechnology **[58]**.

2.2. Polymer structures

Polymers can be classified as linear, branched, or cross-linked polymers depending on their structure.

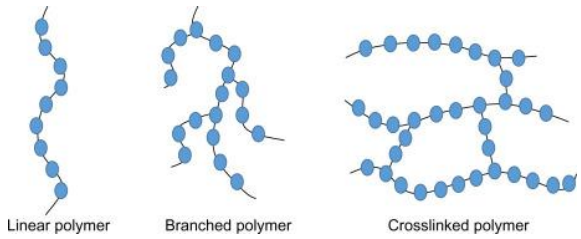

Figure II. 10: Schematic representation of linear, branched, and cross-linked polymers **[59]**.

2.2.1. Linear

Linear polymers are those polymers in which the monomer molecules link together in one continues length to form the polymer molecule **[59]**.

2.2.2. Branched

Branched polymers, polymers with more than two chain ends per molecule, can form in both step and chain polymerizations. Branched polymer molecules are those in which there are side branches of linked monomer molecules protruding from various central branch points along the main polymer chain **[59]**.

2.2.3. Cross-Linked

When polymers are produced in which the polymer molecules are linked to each other at points other than their ends, the polymers are said to be cross-linked. Crosslinking can be made to occur during the polymerization process by the use of appropriate monomers, it can also be brought about after the polymerization by various chemical reactions.

The crosslinks between polymer chains can be of different lengths depending on the crosslinking method and the specific conditions employed **[59]**.

2.3. Polymer synthesis techniques

There are two general types of polymerization reactions: addition polymerization and condensation polymerization **[60]**.

2.3.1. Addition polymerization

Addition polymerization is a process in which unsaturated monomers, such as alkenes, add to each other to form a long-chain polymer without the formation of any by-products. This reaction involves the formation of a free radical or an ionic species, which initiates the polymerization process. Addition polymerization is typically a chain-growth process, where the monomer adds to the end of the growing chain, resulting in a high molecular weight polymer.

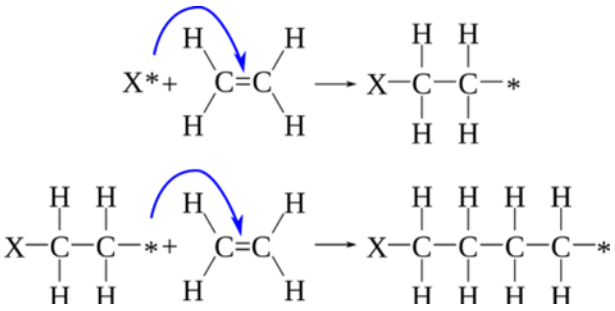

Figure II. 11: Polyethylene synthesis by addition polymerization **[60]**.

2.3.2. Condensation polymerization

Condensation polymerization, also known as step/step-growth polymerization is merely classical organic reaction that is used to produce linear macromolecules starting from bi-functional monomers, with the elimination of a small molecule, typically water or an alcohol. The reaction involves the formation of covalent bonds between monomers and the release of a by-product **[61]**.

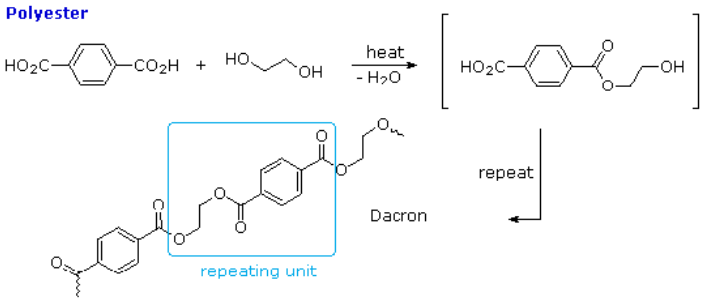

Figure II. 12: Polyester synthesis by condensation polymerization **[60]**.

2.4. Classification of Polymers

Polymers can be classified into three classes, thermoplastics, thermosets and elastomers. The main differences are shown in (Table II.1).

2.4.1. Thermoplastics

Thermoplastics are materials that can be melted and reformed repeatedly through the application of heat, without undergoing any significant chemical changes. This characteristic

makes them ideal for many different applications, including injection moulding, blow moulding, and extrusion processes **[61]**.

2.4.2. Thermosets

Thermosets are formed when two or more components chemically react with each other under ambient conditions or when induced by radiation or heat to form a highly cross-linked network. The formation of thermosets is an irreversible process. Thermosets are typically hard and rigid. They tend to have higher temperature resistance when exposed to heat and will not creep or warp at higher temperatures compared to thermoplastics. Thermosets typically are used for structural applications where high strength and stiffness is required to resist high loads **[62]**.

2.4.3. Elastomers

Elastomers are amorphous materials with a low degree of cross-links, exhibiting rubber-like behavior i.e., high degrees of elastic deformation such that they can deform and stretch under stress, and then return to their original shape after stress is removed. They are widely used in applications such as seals, gaskets, tires, and other products that require flexibility and resilience **[63]**.

Table II. 1: Three main classes of polymer **[64, 65]**.

Thermoplastic	Examples	Thermosets	Examples	Elastomers	Examples
Highly recyclable and reshaping ability	High-density polyethylene	Not recyclable or reshaped	Polyisoprene	High resilience	Polybutadiene
High strength resistance	Polyethermide	Flexible	Polyurethane	Abrasion resistance	Poly chloroprene
Chemical resistance	Polyphenylene oxide	Dimensional stability	Benzoxazines	Good electrical properties	Silicone
More expensive	Polyether ketones	Cost effective	Polyester resin	Cost less	Natural rubber

2.5. Polymer applications

The importance of polymers is due to their wide application range, as they resemble industrial, economical, medical, and academic interests and goods that enhance our lives on a daily basis **[65]**.

Some of its applications are listed below:

- Medicine: Many biomaterials, especially heart valve replacements and blood vessels, are made of polymers like Dacron, Teflon and polyurethane;
- Consumer Science: Plastic containers of all shapes and sizes are light weight and economically less expensive than the more traditional containers;
- Industry: Automobile parts, windshields for fighter planes, pipes, tanks, packing materials, insulation, wood substitutes, adhesives, matrix for composites.

2.6. Polymer properties

The physical, chemical, and mechanical properties of a polymer network depend highly on the density and functionality of the connecting nodes. The properties can be modulated by varying the monomer molecular weight, functionality of the units, and the multifunctional monomer ratio **[65]**.

2.6.1. Thermal properties

In the amorphous region of the polymer, at lower temperature, the molecules of the polymer are in, say, frozen state, where the molecules can vibrate slightly but are not able to move significantly. This state is referred as the glassy state. In this state, the polymer is brittle, hard and rigid analogous to glass. Now, when the polymer is heated, the polymer chains are able to wiggle around each other, and the polymer becomes soft and flexible similar to rubber, this state is called the rubbery state. The temperature at which the glassy state makes a transition to rubbery state is called the glass transition temperature Tg. The glass transition occurs only in the amorphous region, and the crystalline region remains unaffected during the glass transition in the semi-crystalline polymer **[66]**. The glass transition temperature is the property of the amorphous region of the polymer, whereas the crystalline region is characterized by the melting point. In thermodynamics, the transitions are described as first and second order transitions. Glass transition temperature is the second order transition, whereas the melting point is the first order transition **[66]**.

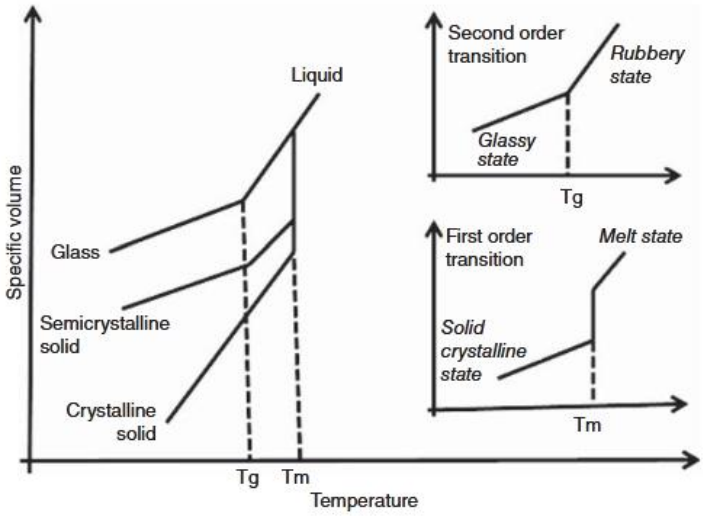

Figure II. 13: Melting point and glass transition temperature of polymer **[66]**.

2.6.2. Physical properties

Physical properties of polymers include molecular weight, molar volume, density, degree of polymerization, crystallinity of material, and so on. Some of these are discussed herewith in the following sections **[67]**.

2.6.2.1. Polymer Crystallinity

The state where the polymer chains exist in parallel position that a polymer can be achieve at a particular temperature. It depends on chemical nature, geometrical structure, molecular weight and molecular weight distribution etc **[67]**.

The polymeric chains being very large are found in the polymer in two forms as follows:

- Lamellar crystalline form: in which the chains fold and make lamellar structure arranged in the regular manner and amorphous form in which the chains are in the irregular manner. The lamellae are embedded in the amorphous part and can communicate with other lamellae via tie molecules,

  amorphous polymer;

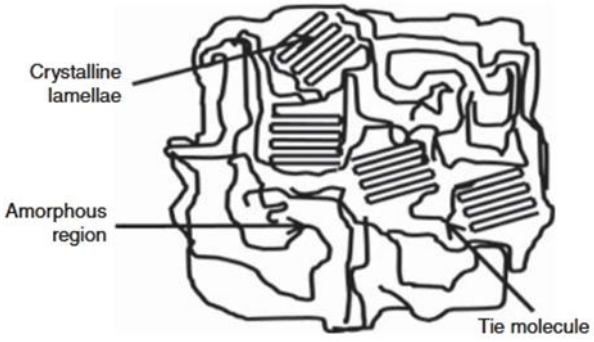

Figure II. 14: Semi-crystalline polymer **[67]**.

- Spherulites: if the molten polymer is cooled down, then the crystalline lamellae grow in radial direction from a nucleus along the three dimensions leading to a spherical structure called spherulite. Spherulite formation and its diameter depend on various parameters such as the number of nucleation sites, polymer molecule structure and rate of cooling. Due to highly ordered lamellae in the spherulite, it shows higher density, hardness, tensile, strength, and Young's modulus **[67]**.

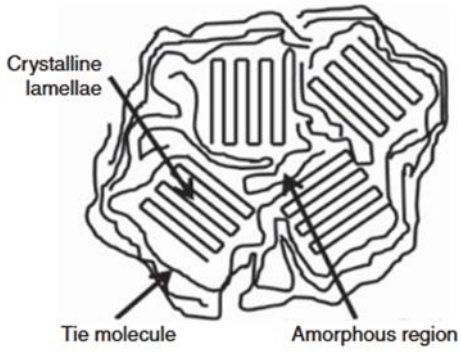

Figure II. 15: A structure of spherulite **[67]**.

2.6.2.2. Degree of Polymerization and molecular weight

The degree of polymerization (DP)-n in a polymer molecule is defined as the number of repeating units in the polymer chain. It is calculated as the ratio of molecular weight of a polymer and molecular weight of the repeat unit. Higher DP is desired for better mechanical properties **[68]**.

$$\text{Degree of polymerization} = \frac{\text{number average molucaler weight}}{\text{Moleculer weight of the repeat unit}} \qquad \textbf{(II.1)}$$

- Molecular Weight Averages: Suppose we have a set of values {x1, x2, …, xn} and the corresponding probability of occurrence is given by {P1, P2, …, Pn}, then the average value is defined as follows:

$$\sum_{i=0}^{\infty} P_i X_i \qquad \textbf{(II.2)}$$

- The number-average molecular weight is given by:

$$Mn = \sum_{i=0}^{\infty} \left[\frac{Ni}{\sum_{j=0}^{\infty} Nj} \right] Mi = \frac{\sum_{i=0}^{\infty} M_i N_i}{\sum_{j=0}^{\infty} N_J} \qquad \textbf{(II.3)}$$

- Weight-Average Molecular Weight:

  The weight-average probability is given by:

$$Pi = \frac{M_i N_i}{\sum_{j=0}^{\infty} N_j M_j} \qquad \textbf{(II.4)}$$

  The weight-average molecular weight is given by:

$$M\omega = \sum_{i=0}^{\infty} \left[\frac{N_i M_i}{\sum_{j=0}^{\infty} N_j M_j} \right] * M_i = \frac{\sum_{i=0}^{\infty} N_i M_i^2}{\sum_{j=0}^{\infty} N_j M_j} \qquad \textbf{(II.5)}$$

2.6.3. Mechanical properties

It is important to be familiar with some basic mechanical properties of the material before its application in any field, such as how much it can be stretched, how much it can be bent, how hard or soft it is, how it behaves on the application of repeated load and so on **[67]**.

2.6.3.1. Strength

The strength is the stress required to break the sample. There are several types of the strength, namely tensile, compressional, flexural, torsional, impact and so on. The polymers follow the following order of increasing strength: linear < branched < cross-linked < network.

Factors Affecting the Strength of Polymers:

- Molecular Weight: The tensile strength of the polymer rises with increase in molecular weight and reaches the saturation level at some value of the molecular weight;
- Crosslinking: The cross-linking restricts the motion of the chains and increases the strength of the polymer;

Crystallinity: The crystallinity of the polymer increases strength, because in the crystalline phase, the intermolecular bonding is more significant **[69]**.

2.6.3.2. Percent Elongation to Break (Ultimate Elongation)

It is the strain in the material on its breakage. It measures the percentage change in the length of the material before fracture. It is a measure of ductility. Ceramics have very low (<1%), metals have moderate (1–50%) and thermoplastic (>100%), thermosets (<5%) value of elongation to break **[67]**.

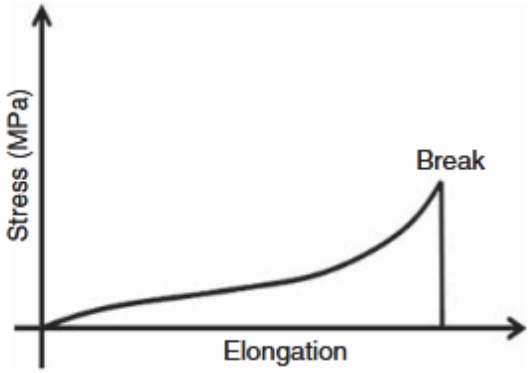

Figure II. 16: Elongation to break of the polymer **[67]**.

2.7. Polymeric nanostructure materials

Polymeric nanostructured materials (PNMs), which are polymeric materials in nanoscale or polymer composites containing nanomaterials, have become increasingly useful for multiple applications **[70]**, for example nanocomposites which have various applications, in our study we used polymer nanoclay composites as a pollutant removal.

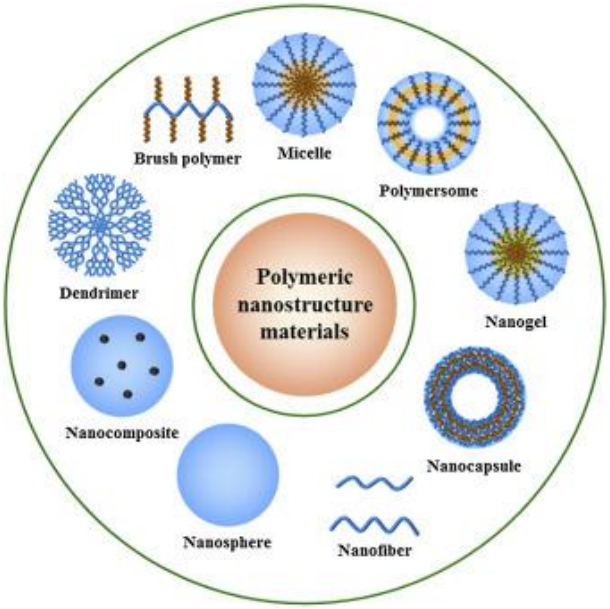

Figure II. 17: Galaxy of nanostructured stimuli-responsive polymer materials **[65]**.

3. Nanocomposites

Nanocomposites have been studied for nearly 50 years, nanocomposites were first referenced as early as 1950, and polyamide nanocomposites were reported as early as 1976. **[71]**. Nanocomposite technology is a newly developed field, in which nanofillers are added to a polymer to reinforce and provide novel characteristics. The most common types of fillers are natural clays, synthetic clays, nanostructured silicas, nanoceramics, nanocalcium carbonates and nanotubes **[72]**. The technological and scientific mastership of nanometric

scale is becoming stronger due to the new research tools and theoretical and experimental developments.

3.1. Morphology of Polymer/clay Nanocomposites

The classification depends on the nature and interaction of the components as well as on the preparation technique. The nature and interaction of the components refers to the type of silicate (clay) material, the organic material used to render the hydrophilic silicates organophilic, and the nature of the polymer matrix **[72]**. Three main types of composites may be obtained when layered clay is associated with a polymer.

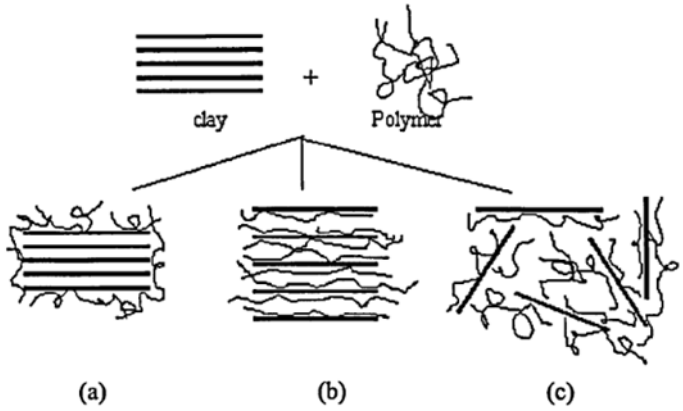

Figure II. 18: Schematic representation of different types of composites (a) Phase separated .microcomposite; (b) intercalated nanocomposite; and (c) exfoliated nanocomposite **[73]**.

3.1.1. Phase-separated structure

When the organic polymer is interacted with inorganic clay, the polymer is unable to intercalate within the clay layers and the clay is dispersed as aggregates or regular stacks of layers formed by stacking together within the polymer matrix. The obtained composite structure is considered "phase separated." The properties of phase-separated polymer–clay composites are in the range of traditional microcomposites **[73]**.

3.1.2. Intercalated nanocomposites

Structures are obtained when polymer chains penetrate deep within the layers of silicate, while still retaining an ordered structure. Theintercalation of the polymer chains into the layer galleries results in the expansion of the distance between the silicate layers. Due to mechanical shearing forces and interactions between the organo-silicates and the polymer chains, the stacks of layered silicates disperse within the matrix, thus increasing the interacting surface area of contact with the polymer **[71]**.

3.1.3. Exfoliated nanocomposites

The exfoliated nanocomposites are obtained when the clay layers are well separated from one another and individually dispersed in the continuous polymer matrix. In this case, the polymer separates the clay platelets by 80–100 Å or more **[73]**.

3.2. Preparation of polymer/clay Nanocomposites

Numerous endeavors have been undertaken to produce intercalated and exfoliated polymer-clay nanocomposites with improved properties. Several polymer characteristics, including polarity, molar mass, hydrophobicity, and reactive groups, as well as clay characteristics such as charge density and modified structure and polarity, influence the intercalation of polymer chains within the clay galleries. As a result, various synthetic methods have been employed for the preparation of polymer-clay nanocomposites. Generally, four preparation methods exist, including in situ template synthesis, solution intercalation, in situ intercalative polymerization, and melt intercalation **[73]**.

3.2.1. In situ template synthesis

The present technique involves the synthesis of clay minerals within the polymer matrix via an aqueous solution (or gel) containing both the polymer and silicate-building blocks, using silica sol, magnesium hydroxide sol, and lithium fluoride as precursors for the clay. The polymer aids in the nucleation and growth of the inorganic host crystals, ultimately becoming trapped within the growing layers. Although this method has potential for promoting dispersion of the silicate layers in a one-step process, it presents serious disadvantages, such as the high temperatures required for clay mineral synthesis which may decompose the polymers, and the aggregation tendency of the growing silicate layers **[73]**.

3.2.2. Solution intercalation

The solution intercalation or method is a process for synthesizing polymer/layered silicate (PLS) nanocomposites. This method involves mixing a preformed polymer solution with clay, using a solvent system in which the polymer or pre-polymer is soluble and the silicate layers are swellable. The nature of solvents is crucial in facilitating the insertion of polymers between the silicate layers. The driving force for the polymer intercalation into layered silicate from the solution is the entropy gained by desorption of solvent molecules, which compensates for the decreased entropy of the confined, intercalated chains. Either the polymer must be polar enough to have positive interaction energy with the surface of the clay or the clay must be organically modified to achieve this goal **[71]**.

3.2.3 In-situ polymerization

The in situ polymerization method, which was the first technique used to synthesize polymer-clay nanocomposites based on nylon 6. The process involves swelling the layered silicate within the liquid monomer or a monomer solution so that polymer formation can occur between the intercalated sheets. Polymerization can be initiated through various means, including heat, radiation, or the diffusion of a suitable initiator or by an organic initiator or catalyst fixed through cation exchange inside the interlayer before the swelling step **[73]**.

3.2.4. Melt intercalation

Melt intercalation is a popular method for preparing polymer/clay nanocomposites, which is advantageous because it does not require solvents. In this method, the layered silicate is mixed with polymer pellets by annealing (either statically or under shear) at a temperature above the softening point of the polymer. As the mixture is heated, the polymer chains diffuse from the bulk polymer melt into the galleries between the silicate layers. The melt intercalation method allows the use of polymers that were previously not suitable for in situ polymerization or solution intercalation **[71, 73]**.

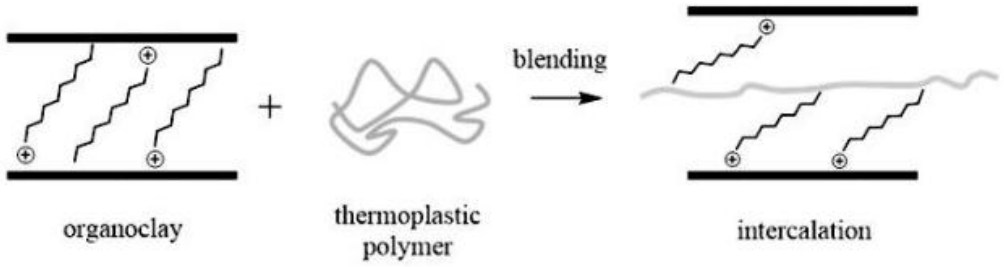

Figure II. 19: Schematic representation of the melt intercalation process **[73]**.

3.3. Applications of Nanocomposites

3.3.1. Wire and cables

The possible use of polymer-clay nanocomposites (PCNs) in wires and cables is due to their improved barrier properties and flame resistance compared to traditional halogenated or non-halogenated flame retardants. Clay minerals in PCNs can reduce the degradation of physical and mechanical properties at the same level of flame retardants or lower the content of flame-retardant substances **[74]**.

3.3.2. Food packaging

Polymer/clay nanocomposites (PCNs) have gained increasing attention in the field of food packaging due to their improved mechanical and barrier properties, making them suitable for various food packaging applications. Additionally, PCNs offer antimicrobial

properties by slowly releasing antimicrobial agents from clay nanoparticles. The use of PCNs in food packaging has potential benefits for shelf life, waste reduction, and sustainability, but further research is needed to fully understand their effects on food safety and human health **[73]**.

3.3.3. Biomedical applications

Polymers, which are the most extensive and highly promising category of biomaterials, are widely used in various medical applications such as tissue engineering, implantation of artificial organ as well as prostheses, ophthalmology, dentistry, and bone repair **[73]**.

3.3.4. Wastewater pre-treatment

Polymer/clay nanocomposites consisting of clay minerals and cationic polymers like polydiallyldimethylammonium chloride (polyDADMAC) have been proven effective in pretreating wastewater. These nanocomposites utilize colloidal neutralization and particle bridging mechanisms, where the cationic polymer neutralizes the negative charge on wastewater particles, while the clay minerals act as a bridge between the polymer chains, resulting in the formation of larger, heavier aggregates that are easier to remove from the wastewater. Studies have demonstrated that these nanocomposites can reduce total suspended solids TSS and chemical oxygen demand (COD) values in one treatment step, indicating potential for more efficient and cost-effective pre-treatment of wastewater **[73]**.

4. Conclusion

This chapter made it possible, through the literature, to present the general theory about clay materials, bentonite and polymer in terms of morphology, structure and properties. Additionally offered were nanocomposites and nanocomposites of the polymer matrix. Thus, this theoretical study demonstrates that clay-based nanocomposites are have the potential to play an important role in the future, due to the possibility of applying them as a more efficient alternative to classical materials, especially in environmental applications such as water treatment. We chose two main lines of research for the rest of our work:

- Development of sodium-montmorillonites/high-density polyethylene nanocomposites;
- Investigating the viability of applying the developed nanomaterials in environmental fields such as organic pollutant adsorption.

PART B:

EXPERIMENTAL STUDY

CHAPTER III:

MATERIALS AND METHODS

This chapter provides an overview of the materials used and the methodology employed in this study.

1. Materials used

- **Electric scale:** Made by Shimadzu **AUW2200** group from Japan;
- **Press:** Manufactured by **CARVER**;
- **Spectrophotometer:** we used a UV visible adsorption spectrophotometer **(Shimadzu AUW2200)**;
- **Optical microscope:** Microscopic characteristics were observed using optical microscopy **(OPTIKA)**;
- **Two roll mill:** to mix the composite polymer/clay **(IQAP LAP)**;
- **Plastometre:** to test the melt flow index of the composite **(mi2.2 GÖTTFERT)**;
- **Infrared spectroscopy (IR):** Infrared spectroscopy was measured by a Fourier transform infrared spectrometer**;**
- **PH-meter:** pH was monitored with a digital pH-meter;
- **Oven:** The Montmorillonite was dried in a **SELECTA** oven;
- **Stirrer:** It was used in the mixture **(LBX)**;
- **Centrifuge machine:** For the separation of the mixture (dye, clay) (**EBA)**;
- **Glassware:** Beakers, Flasks, Pipettes, Erlens, Magnetic bar, Graduated cylinder, spatula, dropper, mortar and pestle, petri dish with cover, stopper, balance, watch glass, thermometer, funnel.

2. Products used

- **Clay**: The bentonite we used is extracted from the ore of Maghnia in the form of small blocks of average diameter of 1 to 10 cm from the practical point of view, it is essential to make it crushed using a mill to reduce its granulometry; in other words to transform it into very fine powder having a diameter between 60-90 μm.

Figure III. 1: Crushed Clay.

- **High density polyethylene HDPE:** High-density polyethylene (HDPE) is produced via the process of natural gas cracking, which generates ethylene gas. In this process, gas molecules undergo polymerization to form polyethylene. The resulting product has a sludgy appearance, and is subjected to molding in order to obtain the desired shape and properties. HDPE is a strong and versatile polymer material that finds applications in various fields.The HDPE powder we used was obtained from CP2K unit in Skikda's industrial zone.

Figure III. 2: HDPE powder.

- **Hydrogen peroxide:** The peroxide used in the purification step is hydrogen peroxide, also known by its raw chemical formula H_2O_2, with a density of 1.4 g/mL and a molar mass of 34 g/mol. The peroxide was used in low proportions to remove impurities, specifically organic matter, from the clay during the purification process.
- **Sodium chloride:** It has a white crystalline appearance with a molar mass of 58.44 g/mol. The latter was used in the cation exchange process of purified bentonite to obtain sodium bentonite.

3. Adsorbent preparation

To achieve our goal, which is the preparation of adsorbents in the form of PS/clay-based films melt mixing, we first need to treat the clay according to specific steps.

3.1. Bentonite Purification

A. Clay grinding

The process of bentonite grinding involves feeding the material into a grinding machine where it is subjected to a series of physical forces such as crushing, shearing, and friction, which gradually reduce the particle size. This process aims to produce a

finely ground powder with a diameter ranging between 60-90 µm suitable for various applications.

B. Clay sieving

It is necessary to sift the ground bentonite, in order to obtain a homogeneous powder whose particles have the same size. This process is carried out by passing the crushed clay through a 200-mesh sieve.

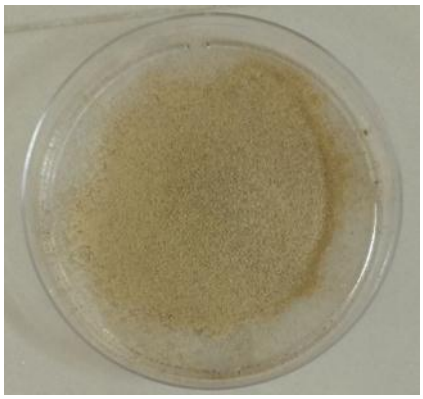

Figure III. 3: Bentonite powder.

C. Purification process

The goal of purification is to obtain a natural bentonite free of all impurities and crystalline phases that it may contain (such as quartz, feldspar, calcite, organic matter, etc.). For this purpose, 30 g of ground bentonite was added to a 1 liter beaker containing a dilute hydrogen peroxide solution (30 mL of 30% hydrogen peroxide), followed by the addition of distilled water until reached the 1000 mL mark with magnetic stirring for 3 h.

Figure III. 4: Magnetic stirrer.

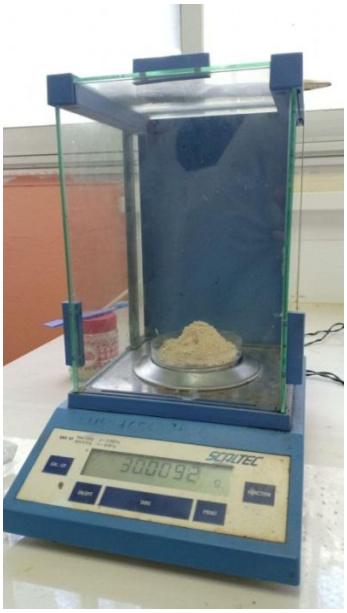

Figure III. 5: Electronic balance.

After retrieving the beakers, each sample were transferred into 1L graduated cylinders and left to settle for an adequate period to facilitate decantation. Following the required decantation time, three distinct phases were observed. The first phase was located at the bottom of the cylinder and consisted of impure clay. The second phase was positioned in the middle of the cylinder and comprised purified clay particles suspended in water. The third phase contained water without any clay content.

The second phase was extracted from each cylinder, and the same process was repeated five times to ensure complete treatment of the entire amount of bentonite. Beakers and test tubes were left to settle for 24 hours, and after settling, water was separated from the clay and the purified clay was recovered. The recovered clay had dried in an oven at 100°C for 24 hours, then we grinded it.

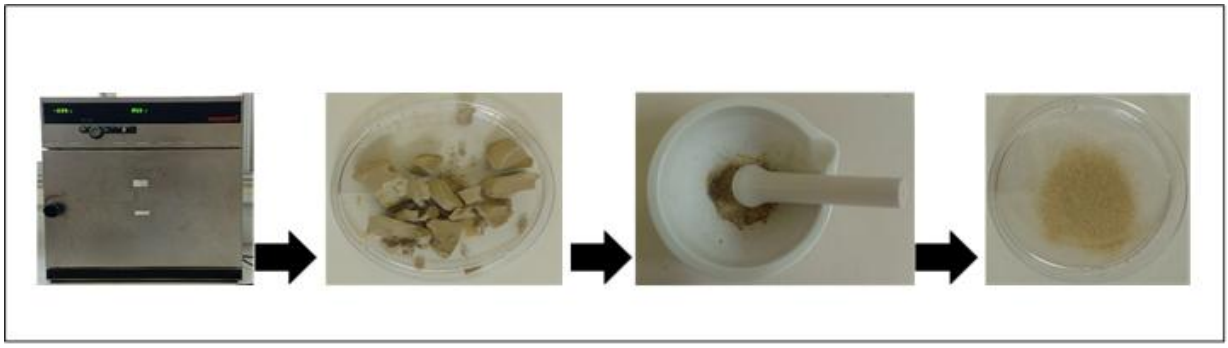

Figure III. 6: Dried Clay Grinding.

3.2. Preparation of sodium montmorillonite

The following steps were followed in order to obtain sodium montmorillonite (MMT-Na);

- 30 g of purified montmorillonite was added to one liter of 0.5 M NaCl solution under stirring for 72 h at room temperature. Then the mixture was left to settle for 24 hours. The clay was then recovered using centrifugation;
- In order to remove all chloride ions (Cl^-), the exchange process follows several consecutive washes from five to six times; so MMT-Na was added to 1 liter of distilled water and stirred for 15 minutes. After stopping stirring, the beaker was left to stand for 15 minutes and the supernatant was separated from MMT-Na.

After ensuring the elimination of all impurities (by silver nitrate test), MMT-Na was washed one last time in 1l of distilled water with stirring for 20 minutes, then it is separated from water by centrifugation and dried in an oven for 24 h at 100°C, then grind it well and then store it in clean, tightly closed bottles, away from any contamination.

Figure III. 7: Centrifuge machine.

3.3. Preparation of HDPE/Clay Nanocomposites

HDPE/Clay nanocomposites were prepared with a weight loading rate of 4% through a melt mixing process. To prepare forms of 150g of HDPE/clay composite, 144g of HDPE and 6g of clay (types 1, 2, and 3) were weighed and mixed. The mixture was dried for 24 hours at 80°C to eliminate any residual moisture that could lead to the formation of air bubbles on the material surface during implementation.

Table III. 1: Different prepared formulas.

Formula	HDPE/Raw-Mmt (1)	HDPE/Treated-Mmt (2)	HDPE/Na-Mmt (3)
HDPE (g)	144	144	144
Clay (g)	6	6	6

The prepared HDPE/clay composites were subjected to melt mixing at a rotation speed of 32 rpm and a temperature of 200°C in a two-roll mill (figure III.8) until complete melting of the polymer and incorporation of the filler. The resulting mixture was shaped into long sheets, which were then cut into small rods of 3 cm in length and crushed into small particles.

Figure III. 8: Two roll mill.

Films were prepared using an automatic hydraulic press (figure III.11) under the following conditions: pressure of 100 kg/cm², temperature of 220°C, preheating for 7 minutes, degassing for 1 minute, and pressure for 15 minutes. The resulting films (figure III.10) were then cut.

Figure III. 9: Hydraulic press.

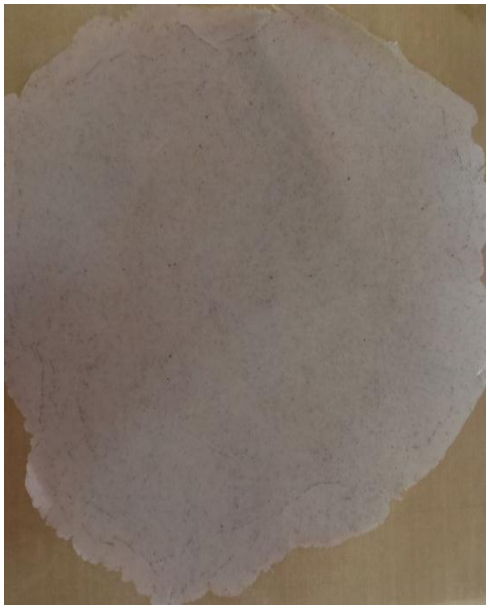

Figure III. 10: Nanocomposites film.

4. Nanocomposites Characterizations

Prior to utilizing the synthesized HDPE/Clay nanocomposites in any application, it is imperative to determine their properties. Therefore, a series of tests were conducted on the composite material.

4.1. Rheological Tests (Melt Flow Index)

The Melt Flow Index (MFI) is a quality control test that measures the flow of a resin through a die. It is the rate of melted polymer in grams, that is extruded through a capillary die in 10 minutes under a specific load. The unit is grams per 10 minutes. The specific mass used to test High density polyethylene resins is 2.16 kg. In general, a high MFI value corresponds to a good processing ability, while a low MFI value indicates polymers with high mechanical strength **[75]**.

This analytical methodology is performed in accordance with the ASTM D-1238 standard. The plastometer apparatus must be heated to a temperature of 190 °C for a minimum of 15 minutes, after which the cylinder should be cleaned and the die installed. To commence the analysis, 2.5 to 3 g of the sample are poured into the cylinder and the piston is inserted under slight pressure. The sample was preheated for 3 minutes without a load and then heated for an additional 3 minutes with a load, and subsequently the extruded part containing air bubbles is severed, enabling the product to flow for 10 minutes. Finally, the mass of the extruded product is determined by weighing it, which corresponds to the MFI of the product in grams per 10 minutes **[75]**.

4.2. Density test

The mass density of a substance, also known as volumetric mass density, is a physical quantity that characterizes the mass of the substance per unit volume. It is the inverse of the specific volume.

On this study, the density was measured using the density method at 23°C using the ASTM D-1505 apparatus **[75]**.

4.3. Optical test

In order to investigate the microscopic characteristics of the film sample, an optical test was conducted using an OPTIKA optical microscope. The sample was first prepared according to the specific requirements of the microscope and desired observation. The microscope was then set up with an x4 objective lens, and the sample was observed through the microscope. A picture of the sample was captured.

4.4. Fourier-transform infrared spectroscopy (FTIR)

The analysis was carried out using a Fourier transform spectroscope, which sends infrared radiation onto the sample and measures the wavelengths at which the material absorbs and the intensity of the absorption.

5. Colorant adsorption

In this part of the work, the solution was prepared and the films nanocomposites were applied to the adsorption process at different parameters.

5.1. Choice of dyes

The choice of dye meets the following criteria:

- ✓ High solubility in water;
- ✓ can be analysed by UV/visible spectrophotometer;
- ✓ Permanent stability.

5.2. Malachite green dyes

Malachite green is an organic chloride salt that is the monochloride salt of malachite green cation. Used as a green-coloured dye, as a counter-stain in histology, and for its anti-fungal properties in aquaculture. It has a role as a fluorochrome, a histological dye, an antifungal drug, a carcinogenic agent, a teratogenic agent, an environmental contaminant and an antibacterial agent. It contains a malachite green cation.

5.2.1. Physicochemical characteristics of the dye Malachite Green

Malachite green (or aniline green, or diamond green B) is a toxic chemical mainly known for its blue-green dye qualities. The name "Malachite Green" comes from the name of a mineral carbonate: Malachite.

An interesting characteristic of Malachite Green is its property as a coloured indicator of pH in chemistry (it has two turning points, one in a very acidic medium and one in a very basic medium). Besides as a dye, as a broad-spectrum toxicant, it has also been used as pesticide and used in textiles.

All its properties are summarized in table (III.2)

Table III. 2: Physicochemical characteristics of malachite green.

Properties	Malachite green dye
Molecular structure	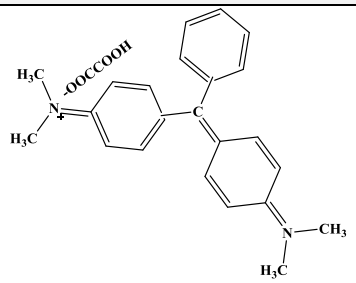
Molecular formula	$C_{23}H_{25}ClN_2$

Color	Blue-green
Molecular weight [g/mol]	364.911
State	Crystals
Solubility in water [mg/dm^3]	High
pKa	10.3
Maximum wavelength [nm]	617
Cas Number	569-64-2

5.3. Preparation of malachite green solution

0.25 g of malachite green dye was dissolved in 250 ml of distilled water to yield a solution of 1 g/L concentration. Subsequent to vigorous agitation, a uniform dark green-blue coloured solution was obtained.

5.4. Determination of the maximum absorption wavelength (λ_{max}) and calibration curve establishing

5.4.1. Spectrophotometry UV-Vis

The maximum absorption wavelength (λ_{max}) was determined by establishing the visible spectrum of a sample solution of 10 mg/L concentration of the dye.

To establish the calibration curve, the absorbance at the maximum wavelength of samples containing dye solutions of various concentrations, prepared from the 1 g/L stock solution was measured.

Then spectrophotometry was used in the next part of the study to calculate the absorbance of the MG solution; each time the spectrophotometry was used, a zero blank of deionized water was placed in the compartment of the equipment

5.5. Experimental protocol

The experimental plan for investigating the adsorption of malachite green dye onto HDPE/MMT films involved varying several factors that could impact adsorption efficiency such as the initial concentration of the dye, contact time, temperature, pH, etc. The objective was to measure the adsorption efficiency of the film for the dye and identify the factors that had the greatest impact on adsorption. By systematically varying these factors and measuring the adsorption efficiency under different conditions, insights were gained on optimizing the conditions to maximize the adsorption efficiency.

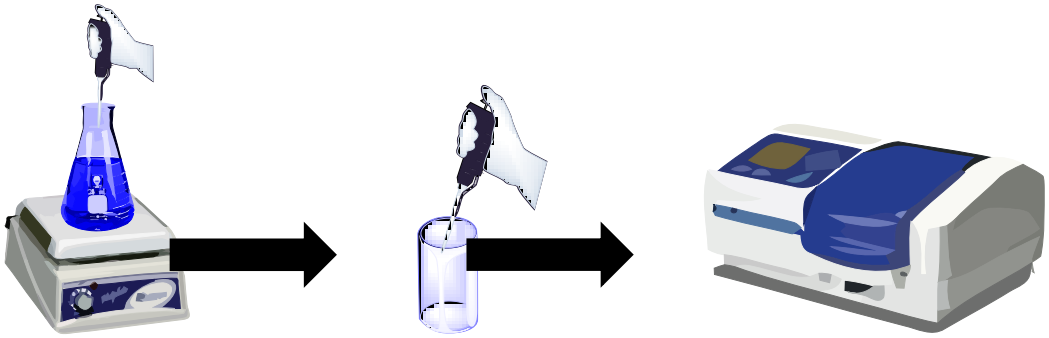

Figure III. 11: Adsorption process setup.

5.5.1. Effect of contact time

To achieve the maximum values of MG adsorption capacity, which represent the saturation of all available active sites on the surface of the adsorbent, we investigated the influence of MG concentration on each adsorbent. The adsorption kinetic for each studied concentration was carried out for a time ranging from 0 to 180 min under the following operating conditions:

- Volume of the MG solution: 100 mL;
- Mass of the adsorbent: 0.2 g.

Samples were taken at predetermined time intervals (5min) for the determination of the MG concentration.

5.5.2. Effect of adsorbent weight

In this study, the influence of mass on the adsorption process was investigated by varying the weight of adsorbent. The aim was to determine the optimal mass of adsorbent required for achieving maximum adsorption efficiency.

5.5.3. Effect of initial concentration of malachite green dye

The effect of the initial concentration of malachite green dye on the adsorption capacity of the adsorbent was investigated through a systematic variation of the initial concentration. The results provide valuable insights into the relationship between the initial concentration and the adsorption capacity, which can inform the optimal selection of adsorbent dosage for practical applications.

5.5.4. Effect of temperature

The effect of temperature on the adsorption capacity on the HDPE/MMTs films for malachite green dye was investigated by varying the temperature of each solution, this

information is important for practical applications of the adsorbent as temperature is a key parameter in real-world scenarios.

5.5.5. Effect of pH

The pH of the solution can have a significant impact on the adsorption capacity of the adsorbent, as it can affect the surface charge of both the adsorbent and the dye molecules.

The pH of the solution was varied from pH 4 to10 and measured the adsorption capacity of the adsorbent at the different pH values, so the optimum pH range for maximum adsorption efficiency can be determined.

5.5.6. Isotherm modelling

Two commonly used isotherms, Freundlich and Langmuir were employed in the present study. The nonlinear Freundlich and Langmuir isotherms are represented by equations (III.1) and (III.2):

$$q_e = K_F C_e^{1/n} \qquad \textbf{(III.1)}$$

$$q_e = \frac{q_m k_L c_e}{1 + k_L c_e} \qquad \textbf{(III.2)}$$

q_e: The amount of dye adsorbed at the equilibrium [mg/g];

C_e: The equilibrium concentration [mg/L];

K_F, 1/n: Freundlich constants, respectively adsorption constant and measure of adsorption intensity;

K_L, q_m: Langmuir constants, respectively adsorption capacity and energy of adsorption.

In order to know the essential characteristics of Langmuir isotherm we calculated the separation factor K_R which is defined by equation (III.3):

$$K_R = \frac{1}{1 + k_L c_0} \qquad \textbf{(III.3)}$$

C_0: The initial dye concentration [mg/L]

We say the isotherm is irreversible when (K_R= 0), favourable (0 < K_R < 1), and unfavourable (K_R > 1).

5.5.7. Kinetics of adsorption (pseudo-first-order, pseudo-second-order)

To investigate the adsorption process of MG, we used Lagergren's pseudo-first-order model (III.4) and Ho's pseudo second order model (III.5), the equations are below:

$$q = q_e\left(1 - e^{-tk_1}\right) \quad \textbf{(III.4)}$$

$$q = \frac{q_e^2 k_2 t}{1 + q_e k_2 t} \quad \textbf{(III.5)}$$

CHAPTER IV:
RESULTS AND DISCUSSION

In this chapter we will present the results of the different characterization techniques used in the study as well as the results of the adsorption of the organic colorant. We begin first by discussing the results obtained during the physical and rheological characterization of HDPE/MMTs by melt flow index and density tests, then we discuss and analyze the results of spectroscopic characterization by Fourier-transform infrared spectroscopy (FTIR) and optical microscope. Next, we will present the results of malachite green adsorption tests. We will also describe the adsorption on (HDPE/Na-MMT) using linear models from Langmuir and Freundlich.

1. Characterization

1.1. Melt Flow Index (MFI)

Table IV. 1: MFI test results

Sample	HDPE	HDPE/Raw-MMT(bentonite)	HDPE/Treated-MMT	HDPE/Na-MMT
MFI (2.16 kg/190°C)	0.35	0.11	0.09	0.05

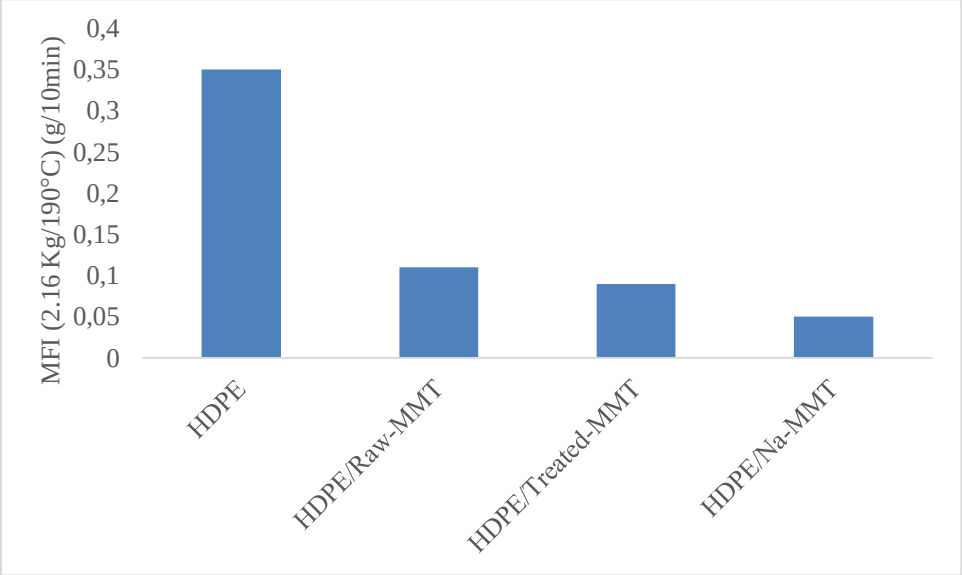

Figure IV. 1: Graph of the melt flux index variation of the nanocomposites.

According to the results of Table IV.1and Figure IV.1, compared to the virgin polymer, a decrease occurred in the MFI values of the nanocomposites after the addition of MMTs. These results indicate that MMT acts as filler in the HDPE matrix, where it acts as a physical barrier to the flow of the HDPE melt during processing i.e. formation of fillers between the polymer segments that hinder the slide of the segments over each other easily, and this can increase the viscosity and reduce the MFI. It can be seen that the

processes of purification and cation exchange that the bentonite was subjected to led to a gradual reduction in MFI values of the nanocomposites, which indicates a change in the crystalline structure and morphology of HDPE.

1.2. Density

Table IV. 2: Density test results.

Sample	HDPE	HDPE/Raw-MMT	HDPE/Treated-MMT	HDPE/Na-MMT
Density (g/cm3)	0.955	0.9645	0.9641	0.9638

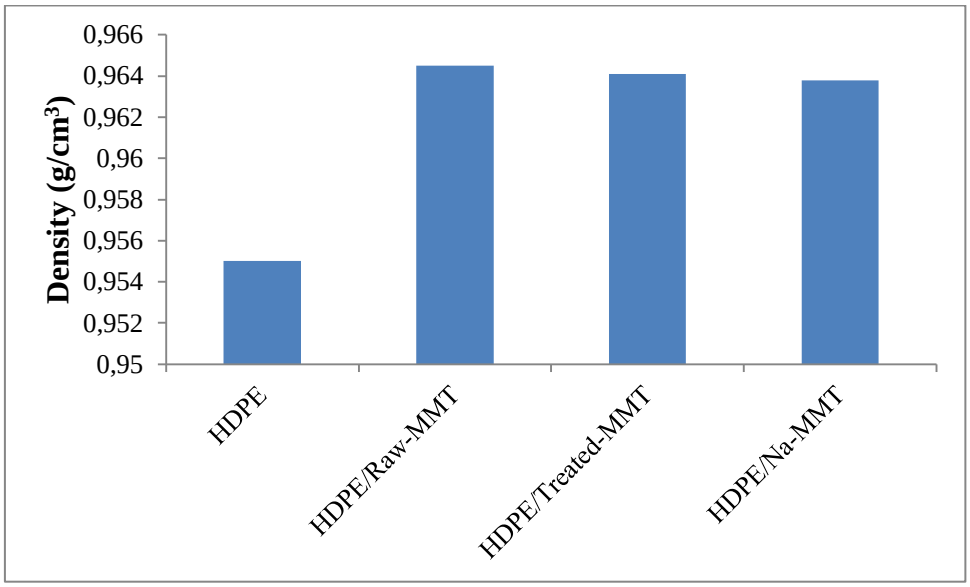

Figure IV. 2: Density variation of nanocomposites compared to the pristine matrix.

Table IV.2 and Figure IV.2 demonstrates that the incorporation of MMT into HDPE leads to a small increase in density with the range of 0.01 due to the addition small quantity of MMT. This can be attributed to the reduction in free volume within the polymer matrix. Additionally, MMT itself possesses a higher density compared to polyethylene, and the presence of MMT particles contributes to the overall mass of the composite material.

We can observe a decrease in density in the case of HDPE/Treated-MMT and HDPE/Na-MMT compared to HDPE/Raw-MMT. This phenomenon can be attributed to the elimination of impurities during the treatment process.

1.3. Optical microscope

The observations using optical microscope were conducted on nanocomposites, as depicted in (Figure IV.3).

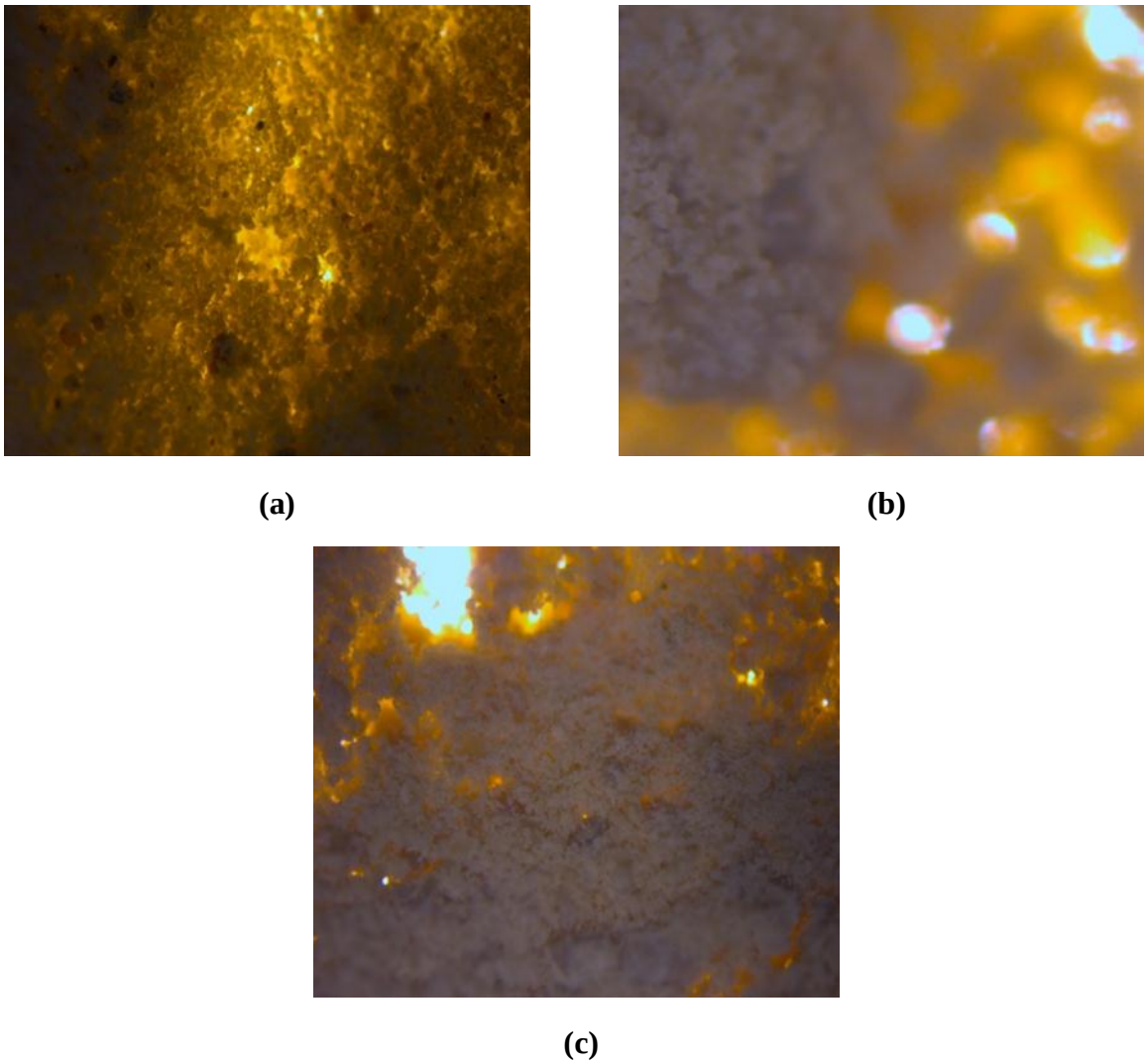

Figure IV. 3: Optical microscope images; (a) bentonite (Raw-MMT), (b) Treated-MMT and (c) Na-MMT.

Figure IV.3 shows optical microscope images of different clays. From natural bentonite image, different aggregates with shapes ranging from spherical to semi-spherical with unequal sizes can be observed. It can also be noted the presence of black and dark-brown impurities in the form of large micrometer-scale granules.

Purification of bentonite resulted in pure-MMT particles (Figure IV.3.b) with a spherical shape and near sizes, free from impurities, and a color change from yellowish-white brown.

There is no noticeable difference between the purified-montmorillonite and Na-montmorillonite images (Figure IV.3.b, c), indicating that the cation exchange process

occurs at the primary particle level, where the intercalation of sodium cations (Na+) in the galleries, which increases the interfoliar distance. Light microscope images confirm that montmorillonites are a porous material with nanometer-sizes pores capable of adsorbing cationic pollutants from water.

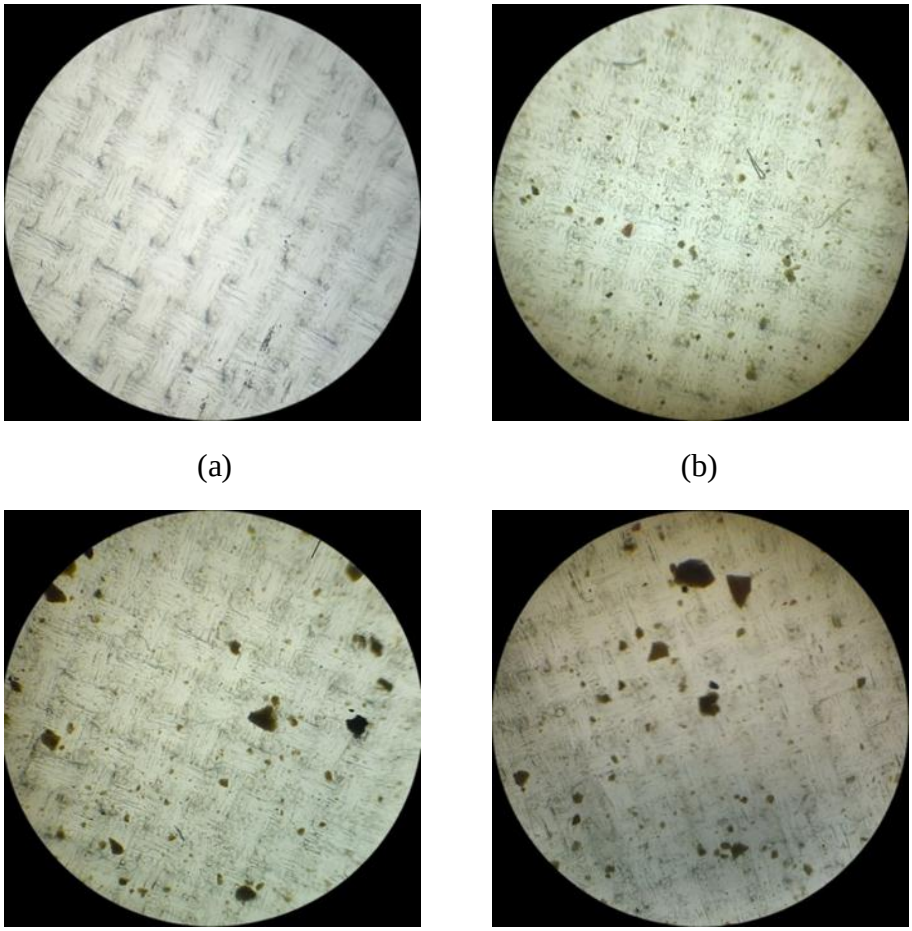

(a) (b)

(c) **(d)**

Figure IV. 4: Optical microscope observation (a) HDPE; (b) HDPE/Raw-MMT; (c) HDPE/Treated-MMT; (d) HDPE/Na-MMT.

According to figure IV.4, before adding MMT particles to the HDPE matrix, the microscopic analysis of the HDPE film shows a homogenous and smooth surface. The film appears to be composed of a continuous HDPE matrix with no discernible inclusions or irregularities. After incorporating MMT particles into the HDPE matrix, the microscopic analysis reveals distinct changes in the film's morphology. Small MMT particles are observed dispersed throughout the HDPE matrix, resulting in a heterogeneous surface. The presence of MMT particles introduces visible variations in colour.

After introducing purified MMT particles into the HDPE matrix, microscopic examination reveals noticeable changes in the film's structure. The purified MMT particles are uniformly dispersed within the HDPE matrix, resulting in a finely distributed pattern. The sodium MMT particles are observed within the HDPE matrix, but their dispersion and distribution may vary. In some regions, larger aggregates or clusters of sodium MMT particles may be present, indicating a relatively poor dispersion within the HDPE matrix. These aggregates may contribute to a non-uniform surface with localized areas of higher particle concentration.

Overall, the microscopic analysis before and after adding MMT particles to the HDPE matrix provides visual evidence of the structural changes and the distribution of MMT particles within the film, allowing for a better understanding of the composite morphology and interfacial interactions.

1.4. Fourier-transform infrared spectroscopy (FTIR)

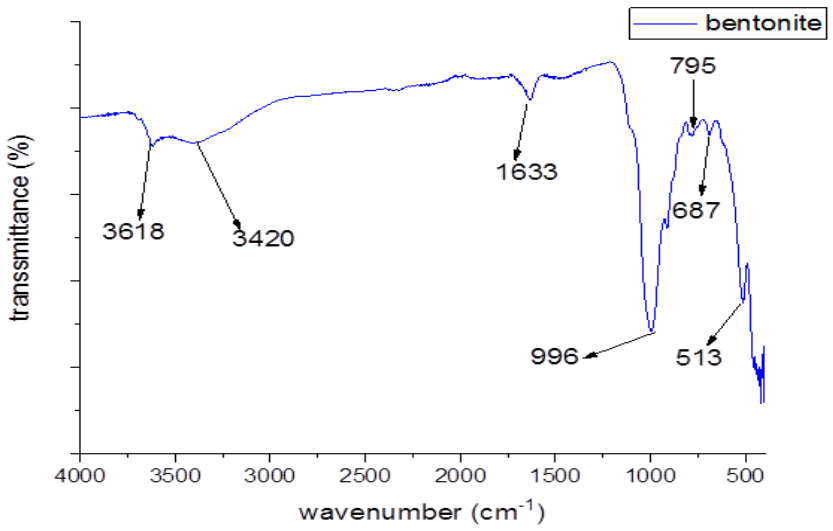

Figure IV. 5: FTIR spectra for Raw-MMT.

The different characteristic peaks of the raw bentonite have been represented in Figure IV.5 and concluded as follow:

- The stretching vibration band at 3618 cm^{-1} is attributed to structural OH groups (interlayer water molecules);
- The band at around 3402 cm^{-1} is assigned to the stretching vibration of water OH;
- The band at 1633 cm^{-1} is attributed to the deformation mode of water OH;

- A broad band appeared at 996 cm^{-1}, corresponding to the Si-O vibration of the tetrahedral layer of bentonite;
- Absorption at 513 cm^{-1} indicates the bending vibrations of Si-O-Al (where Al is an octahedral cation);
- The spectra of natural bentonites show the presence of non-smectitic phases in the samples. The bands at 795 and 687 cm^{-1} indicate the presence of quartz and a mixture of amorphous silica. The band at 795 cm^{-1} is attributed to the lamellar form of disordered tridymite, and 687 cm^{-1} corresponds to the quartz content.

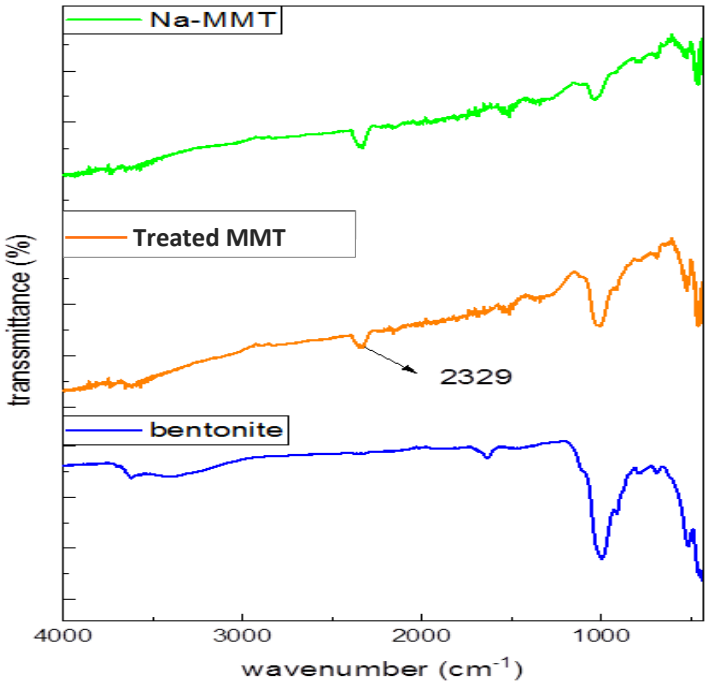

Figure IV. 6: FTIR spectra for Raw-MMT (bentonite); Treated-MMT; Na-MMT.

Figure IV.6 shows the FTIR spectra of treated MMT and sodium MMT, where compared to raw bentonite, a shift in the absorption bands can be observed, accompanied by the appearance of absorption bands at different positions:

- The stretching vibration band of OH groups at 3618 cm^{-1} (in bentonite) shifted to 3649 cm^{-1} in the MMT samples. This is due to the symmetric stretching of OH groups linked to octahedral Al^{3+} cations;
- A new absorption peak appeared at 2329 cm^{-1}, which is attributed to the stretching vibrations of the Si-H silane;
- The stretching bands of Si-O and Si-O-Al at 996 and 513 cm^{-1}, respectively, in raw bentonite increased to 1003 and 517 cm^{-1}, respectively, after treatment;

- The complete disappearance of absorption bands at 795 and 687 cm^{-1} confirms the successful purification process and the obtaining of MMT free from non-smectitic phases.

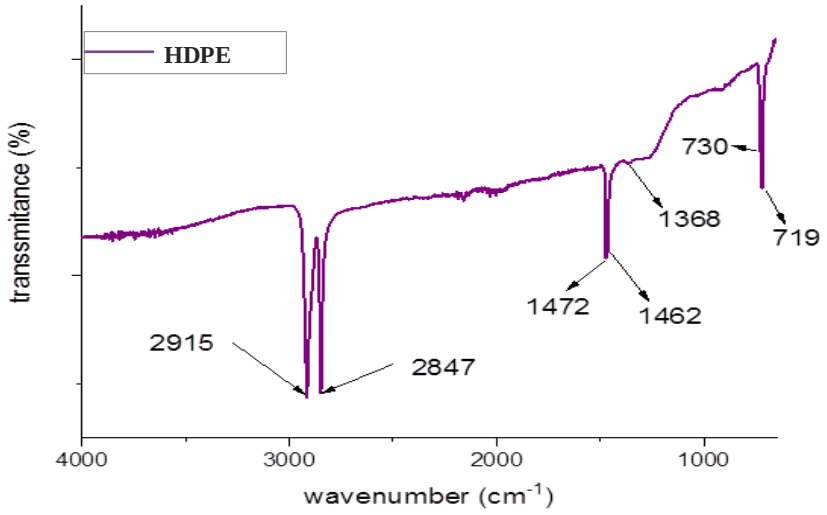

Figure IV. 7: FTIR spectra for HDPE.

According to Figure IV.7, the spectra of pure high-density polyethylene (HDPE) exhibit several characteristic absorption bands:

- A strong absorption band located at 2915 cm^{-1} is associated with the asymmetric stretching vibrations of CH2 groups;
- At 2847 cm^{-1}, there are symmetric stretching vibrations of CH_2 groups (valence vibrations of -CH2- groups);
- The band at 1472 cm^{-1} corresponds to the asymmetric deformation vibration of -CH_2- groups in the crystalline phase;
- At 1462 cm^{-1}, there is a shear vibration of C-H bonds in -CH_2 groups in the amorphous phase;
- The band at 1368 cm^{-1} represents the bending and rocking vibrations of CH_2 groups;
- At 730 cm^{-1}, there are bending vibrations of C-H bonds in -CH_2 groups in the crystalline phase;
- The band at 719 cm^{-1} corresponds to bending vibrations of C-H bonds in -CH_2 groups in the amorphous phase.

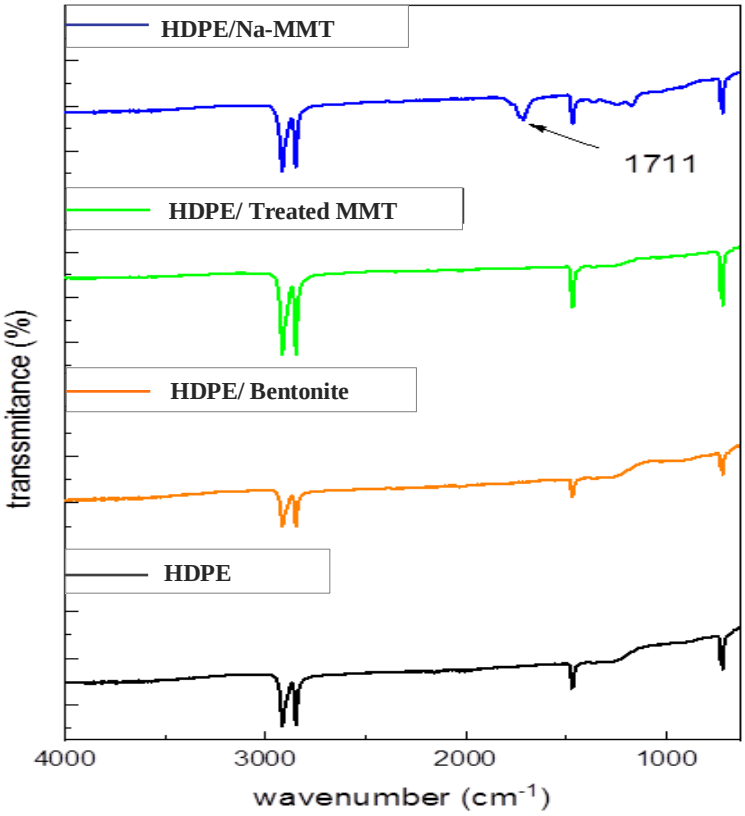

Figure IV. 8: FTIR spectra for the 4 types of nanocomposites.

Compared to the pristine matrix, there were no changes observed in the infrared spectra of HDPE/MMT nanocomposites (using three types of clay) at clay content of 4% by mass. This can be attributed to the low filler content, which preserves the polymer's structure. However, the FTIR spectrum of HDPE/Na-MMT, exhibited the emergence of a new absorption band at 1711 cm^{-1}, which is associated with the formation of Si-C bonds.

2. Spectrophotometric measurement of malachite green solutions

2.1. Maximum absorption wavelength (λ_{max})

The maximum absorption wavelength (λ_{max}) was determined by establishing the visible spectrum of a sample solution with a dye concentration of 10 mg/L. The obtained value for λ_{max} was 617 nm.

2.2. Plotting calibration curve

At a wavelength of 617 nm, we established the calibration curve for malachite green, which provides the absorbance (Abs) as a function of concentration.

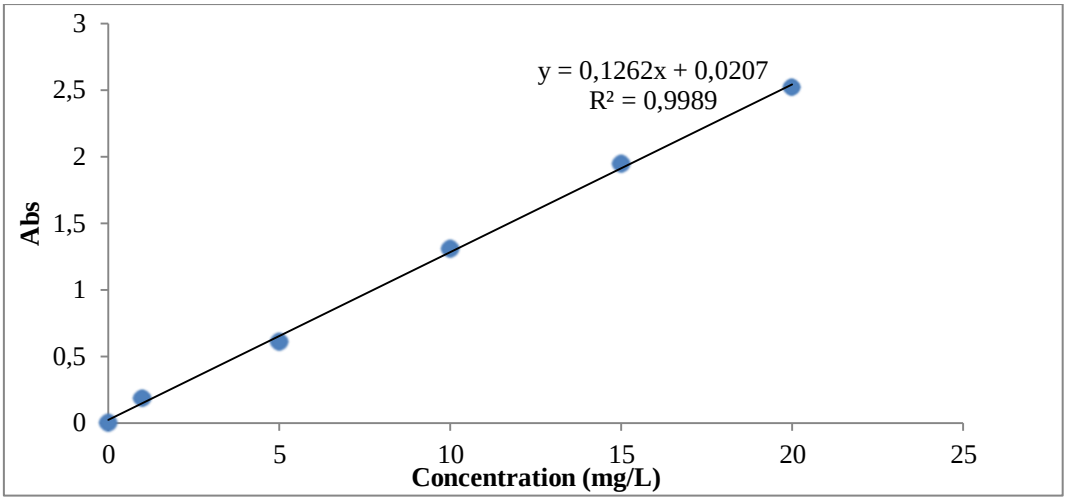

Figure IV. 9: Calibration curve for malachite green solution.

The experimental data indicates a linear relationship between absorbance and concentration, with determination coefficient exceeding 99.8%.

3. Malachite green adsorption

3.1. Contact time effect

The investigation into the adsorption of MG dye by HDPE/MMT nanocomposite films necessitates the assessment of contact time. This refers to the duration required for adsorption equilibrium to be reached, indicating the point at which the adsorbent becomes saturated with the dye. The findings from the experiment are illustrated in Figure (IV.10)

The results obtained from this experiment reveal that our adsorbent is responsible for the decrease in pollutant concentration in the aqueous solution. The graph illustrates that the adsorption rate is initially rapid and gradually slows down as saturation is approached. After 90 minutes of the adsorption process, the final concentration of the dye shows no significant variation. This indicates that equilibrium can be assumed to be reached within this timeframe (90 minutes). The reason behind this behaviour is primarily attributed to the saturation of active sites, which prevents further adsorption from occurring. In addition, we observe that HDPE/Na-MMT had better adsorption performance.

The HDPE had insignificant adsorption, basically HDPE do not have an adsorption capacity. This prove that the addition of MMT to matrix of HDPE give it the capacity of adsorption.

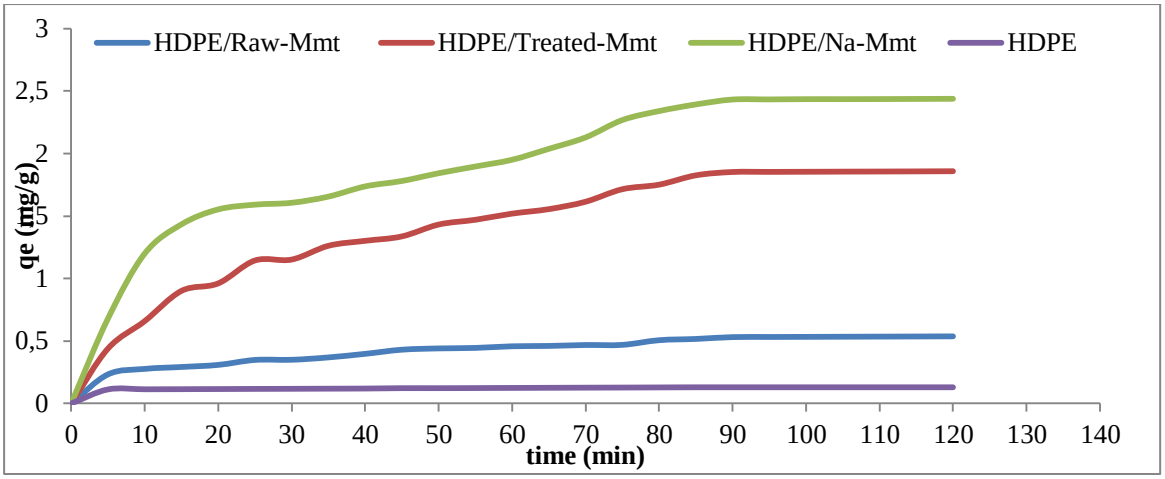

Figure IV. 10: Contact time effect on malachite green adsorption using HDPE and HDPE/MMT nanocomposites (m= 0.2 g; V=0.1 L; C0= 20 mg/L**).**

3.2. Weight effect

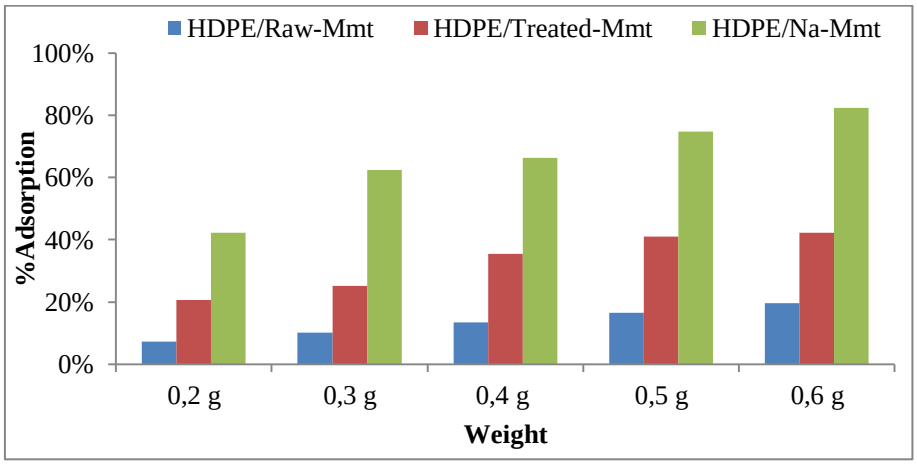

Figure IV. 11: Rate of MG adsorption.

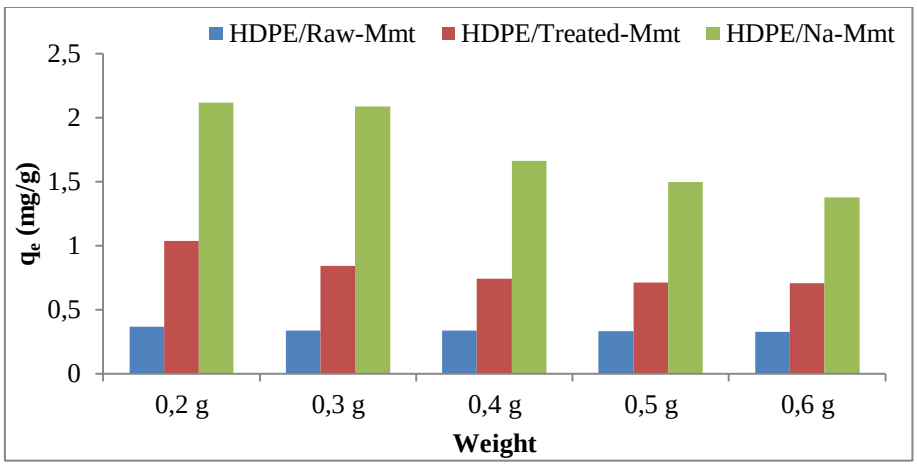

Figure IV. 12: Quantity adsorbed of MG adsorption.

Figure IV.11 and Figure IV.12 display the results of weight influence on adsorption process. It is observed that as the weight of the adsorbent increases for all three nanocomposites, the rate of adsorption also increases. However, there is a decrease in the quantity of dye adsorbed. Furthermore, it is evident that the HDPE/Na-MMT nanocomposite exhibits a superior adsorption rate, with an 82% adsorption rate observed at 0.6 g. additionally, the quantity of dye adsorbed is higher for HDPE/Na-MMT, with a value of 2.11 mg/g at 0.2 g, compared to the other nanocomposites.

3.3. Initial concentration effect

This study and all the rest of batch equilibrium studies were carried out by adding a fixed amount of the three adsorbents (0.6 g) into 50 ml.

As illustrated in Figure IV.13, an increase in the initial concentration range (5-50 mg/L) resulted in a corresponding increase in the q_e values observed, ranging from 0.32 mg/g to 1.53 mg/g. similar trends can be observed in Figure IV.14 and Figure IV.15, where the qe values exhibit an upward trend with increasing initial concentrations. In Figure IV.14, the qe values range from 0.27 mg/g to 1.82 mg/g, while in Figure IV.12, the qe values range from 0.33 mg/g to 2.30 mg/g.

These findings demonstrate a positive correlation between the initial concentration of the adsorbate and the resulting qe values, indicating that higher initial concentrations lead to higher levels of adsorption. This phenomenon can be explained by the fact that driving force increase with augmentation of concentration.

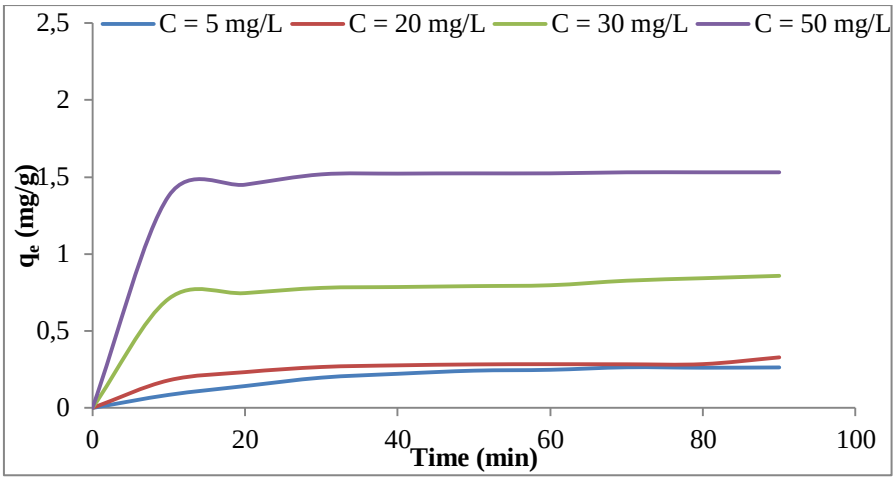

Figure IV. 13: Initial concentration effect of MG adsorption on HDPE/Raw-MMT.

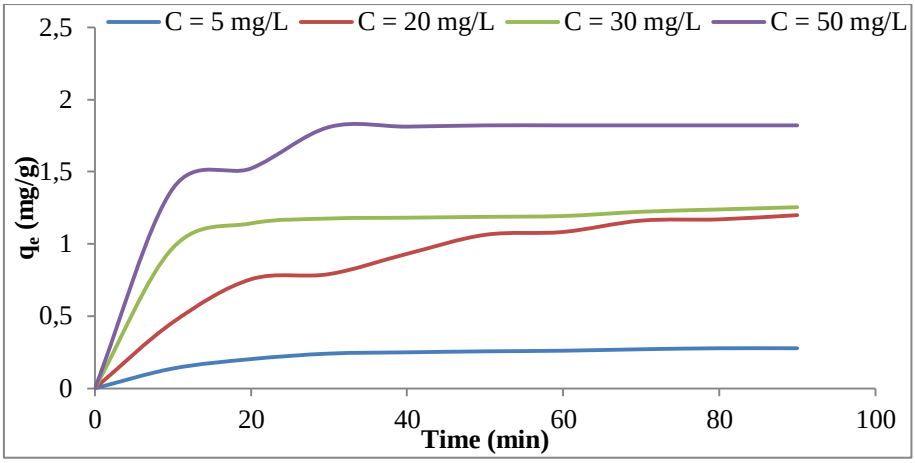

Figure IV. 14: Initial concentration effect of MG adsorption on HDPE/Treated-MMT.

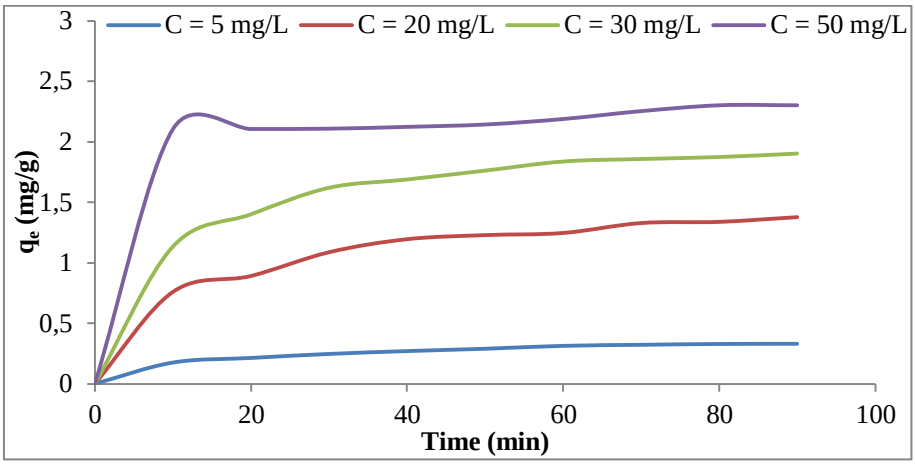

Figure IV. 15: Initial concentration effect of MG adsorption on HDPE/Na-MMT.

Based on the observations depicted in Figures IV.13, IV.14, and IV.15, a similar trend is observed in the adsorption results of the HDPE/Na-MMT nanocomposites as previously observed in the weight effect analysis. Specifically, it can be noted that the HDPE/Na-MMT nanocomposites exhibit a higher adsorbed quantity compared to other composite systems. This can potentially be attributed to the increased contact surface area resulting from the addition of sodium to the MMT particles. The enhanced surface area facilitates a greater interaction between the adsorbate and the composite, leading to a higher adsorption capacity in the HDPE/Na-MMT nanocomposites.

3.4. Temperature effect

The concentration was fixed at 20 mg/L.

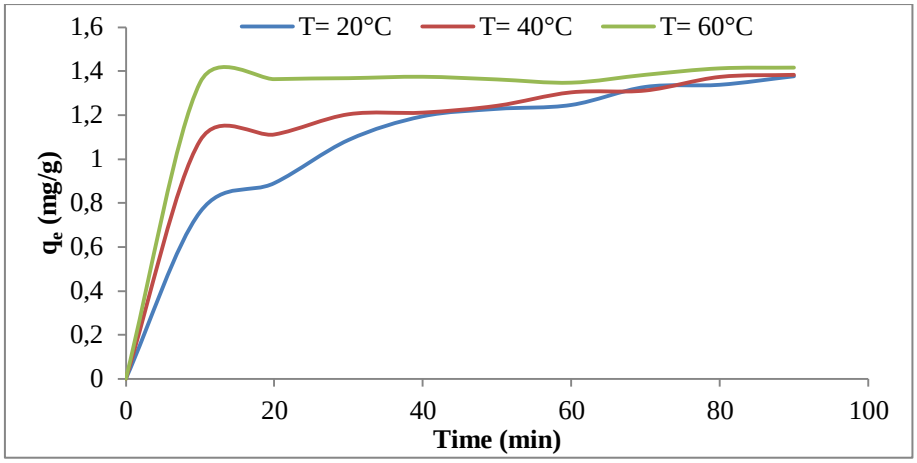

Figure IV. 16: Temperature effect of MG adsorption on HDPE/Na-MMT.

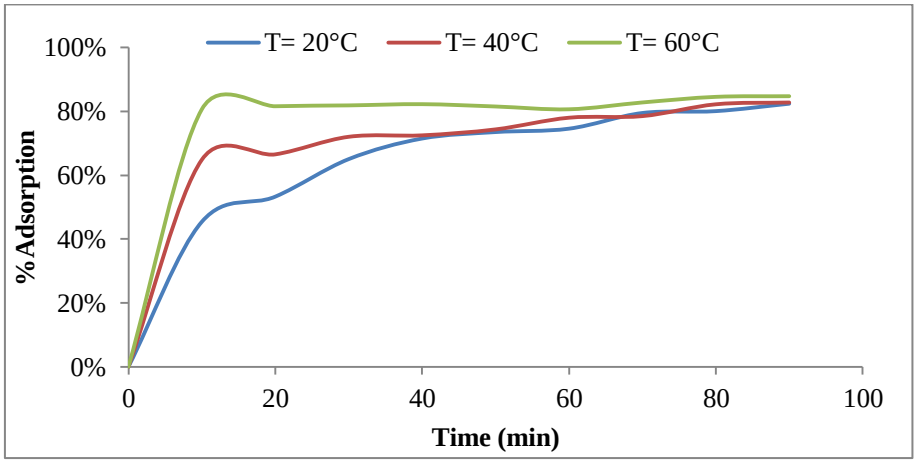

Figure IV. 17: MG adsorption rate on HDPE/Na-MMT.

According to Figure IV.16 and Figure IV.17 we observe that the higher the temperature, more quantity was adsorbed. This augmentation stills insignificant between the chosen temperatures 20°C to 60°C. Indeed we have small increase in the quantity of adsorption from 1.37 mg/g to 1.42 mg/g corresponding to a rate of MG adsorption 82.38% to 84.73%. Also the adsorption kinetics is faster at higher temperature.

In light of the available researches, it is widely acknowledged that the addition of sodium (Na) to montmorillonite (MMT) enhances its properties, including the adsorption capacity, also according to our previous observations indicating the superior performance of HDPE/Na-MMT. Even that we conducted an analysis of the temperature effect on the other two types: HDPE/Raw-MMT and HDPE/Treated-MMT. This additional investigation aimed to explore and evaluate their respective performances, thus complementing the overall study.

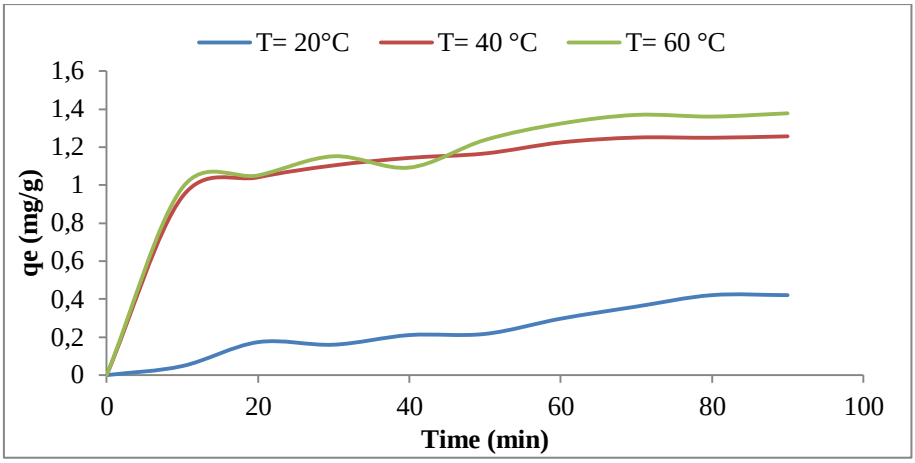

Figure IV. 18: MG adsorption rate on HDPE/Raw-MMT.

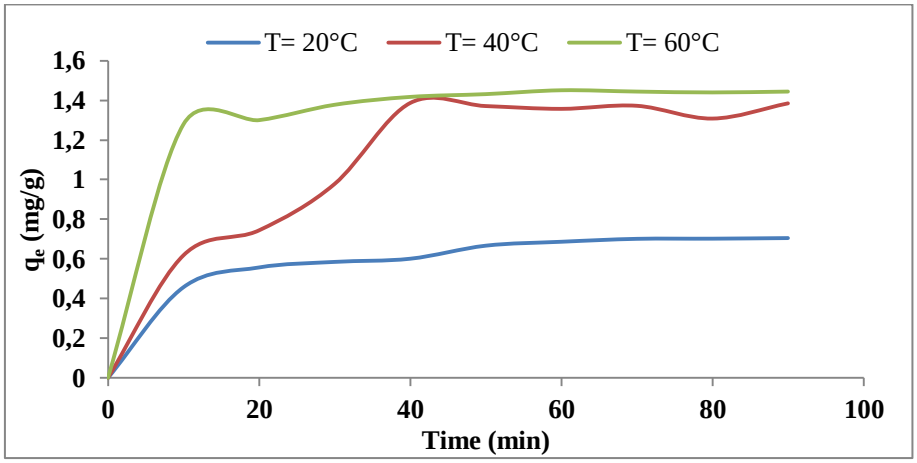

Figure IV. 19: MG adsorption rate on HDPE/Treated-MMT.

Figures IV.18 and IV.19 demonstrate similar trends to Figure IV.16, indicating consistent patterns. However, it is worth noting that undesired desorption occurred at certain points during the analysis. This unexpected phenomenon is regarded as unfavourable. The temperature had a clear effect on the adsorption of HDPE/Raw and HDPE/ treated more than HDPE/Na. The adsorption was the same for different T values on HDPE/Na but for the other two adsorbents at lower T the quantity adsorbed is small compared the quantity adsorbed at higher T. Also at a higher Temperature (> 30) the 3 adsorbents give the same results

These findings suggest that the adsorption of MG is favourable at higher temperatures, indicating an endothermic adsorption mechanism. The increased temperature enhances the mobility of molecules, facilitating their fixation on the surface of HDPE/MMT and resulting in improved efficacy of adsorption. It is noteworthy that the addition of Na to the MMT provides thermal stability; a thermally stable adsorbent

material retains its affinity for the adsorbate molecules and maintains effective adsorbate-adsorbent interactions, even at higher temperatures.

3.5. pH effect

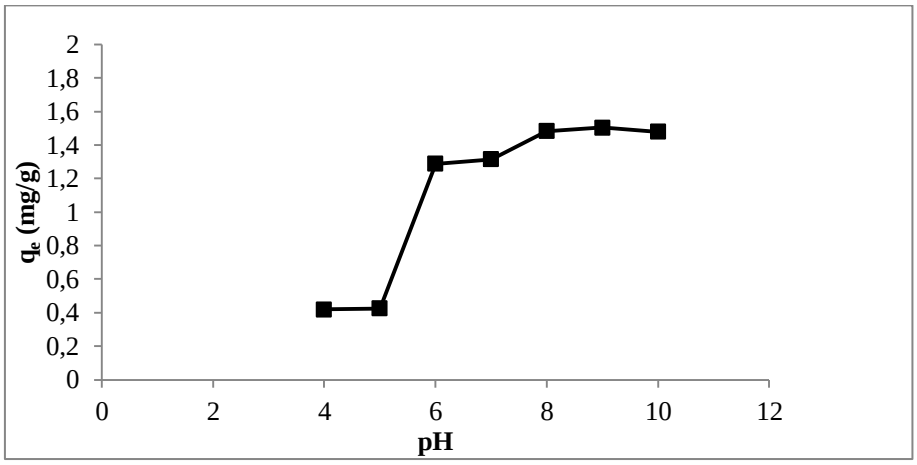

Figure IV. 20: Effect of pH on MG adsorption using HDPE/Na-MMT.

The pH significantly affected the adsorption capacity of MG. As shown in Figure IV.20, the equilibrium sorption capacity was minimum at pH 4 (0.42 mg/g) and increased at pH 6 (1.28 g/mg). More increase was noticed at pH 7-10; reached (1.50 g/mg).

The weak sorption capacity at low pH can be explained by the fact that at acidic pH, H^+ may compete dye ions for the adsorption sites of adsorbent. At high pH the HDPE/Na-MMT may get negatively charged which enhances the adsorption of positively charged dye cations through electrostatic forces of attraction. Therefore a change of solution pH affects the adsorbent surface, such behaviour leads to a shift in equilibrium characteristics of adsorption process.

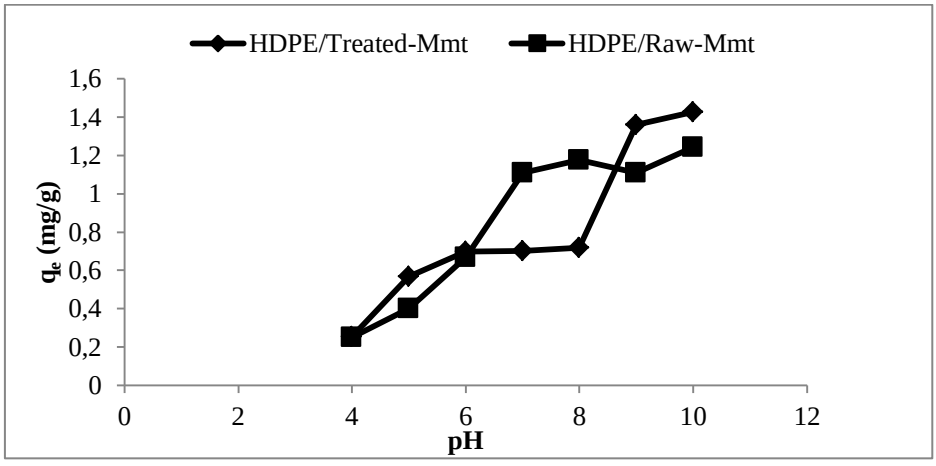

Figure IV. 21: Effect of pH on MG adsorption using HDPE/Treated-MMT and HDPE/Raw-MMT.

Figure IV.21 revealed comparable trends to the pH effect observed in the adsorption of MG on HDPE/Na-MMT (Figure IV.20).

The pH significantly affected the adsorption capacity of MG. As shown in Figure IV.21, for HDPE/Raw-MMT and HDPE/Treated-MMT the equilibrium sorption capacity respectively was minimum at pH 4 (0.25 mg/g; 0.26 mg/g) and increased at pH 6 (0.66 mg/g; 0.70 mg/g). More increase was noticed at pH 7-10; reached (1.24 mg/g; 1.42 mg/g).

4. Adsorption isotherm models

HDPE/Na-MMT nanocomposite was chosen because it showed better performance.

The description of adsorption (on HDPE/Na-MMT) isotherms was released using the linear models of Langmuir and Freundlich.

Table IV. 3: Isotherms constants for MG adsorption on HDPE/Na-MMT.

Langmuir isotherm		**Freundlich isotherm**	
q_m	2,81 ± 0,261	n	2,50 ± 0,696
K_L	0,23 ± 0,063	K_F	0,71 ± 0,203
R^2	0,977	R^2	0,902

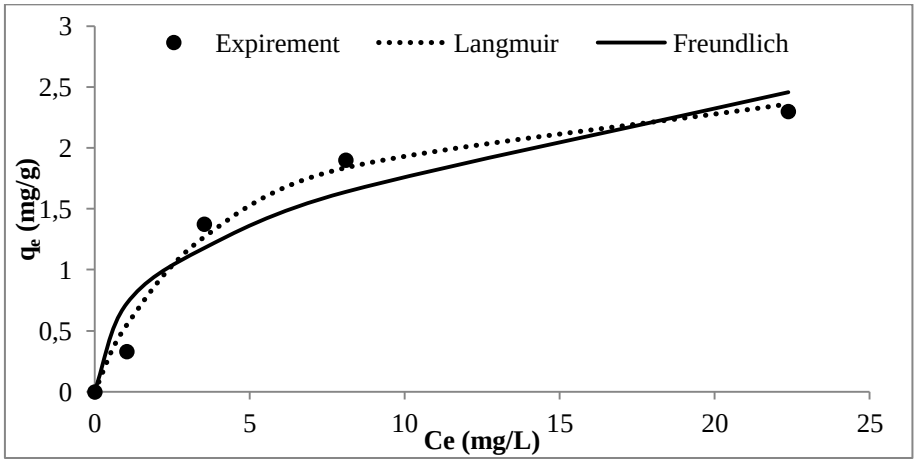

Figure IV. 22: Isotherm plots of MG adsorption on HDPE/Na-MMT.

Table IV.3 shows isotherms parameters and the coefficient of determination R^2, the fitted equilibrium data in Langmuir and Freundlich isotherms are shown in Figure IV.22. We can see in Figure IV.22 that the Langmuir isotherm fits the data better than Freundlich isotherm, also Table IV.3 shows that the value of R^2 Langmuir (0.977) is

higher compared to the value of R^2 in case of Freundlich (0.902) and this tells that the adsorption of MG takes place as monolayer adsorption onto a homogeneous surface.

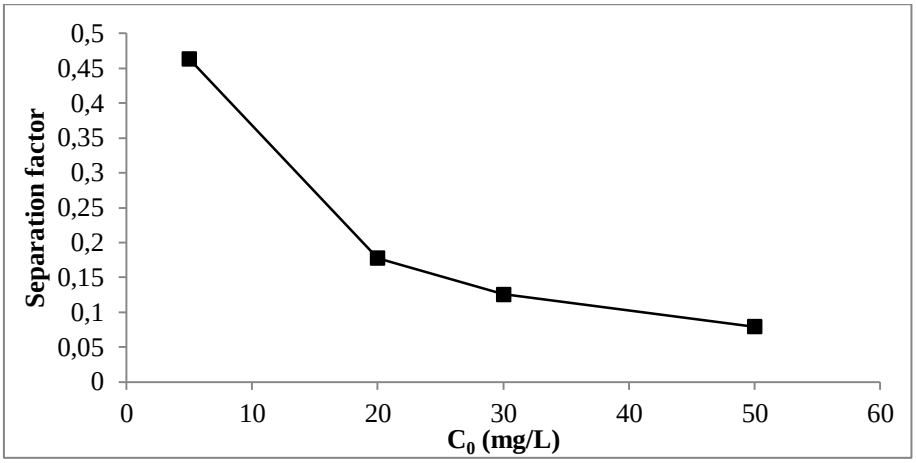

Figure IV. 23: The separation factor for MG adsorption.

For adsorption on HDPE/Na-MMT, $K_{R,}$ values obtained are shown in Figure IV.23 The K_R values are in the range of 0.079-0.463, it indicates that the adsorption is favourable process and shows us the adsorption is nearly irreversible at high concentration.

5. Adsorption kinetic models

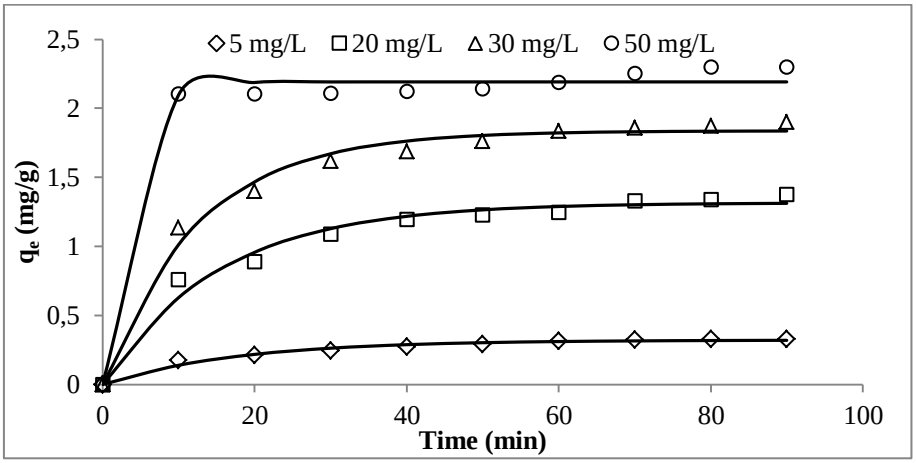

Figure IV. 24: Pseudo first-order model for MG on HDPE/Na-MMT for different initial concentration

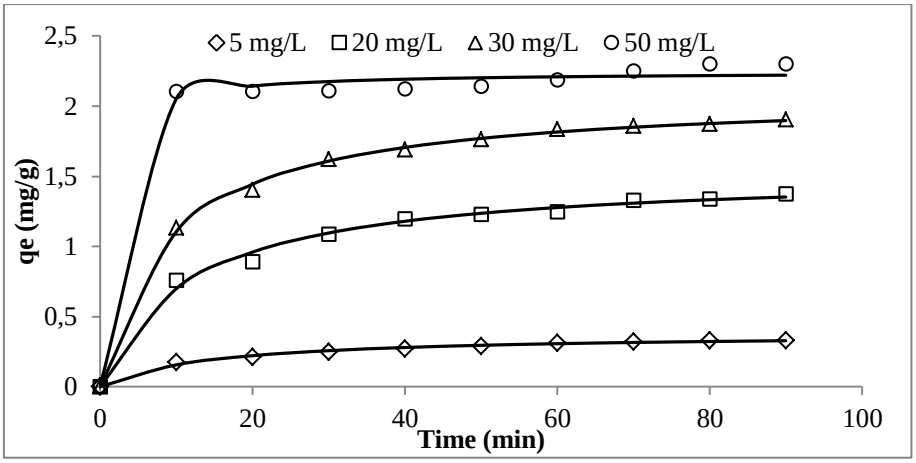

Figure IV. 25: Pseudo second-order model for MG on HDPE/Na-MMT for different initial concentration.

The experimental kinetic results were subjected to nonlinear regression. The outcomes of the fitting process are illustrated in Figures IV.24 and IV.25, while the estimated parameter values can be found in Table IV.4. The depicted figures indicate that the rate of adsorption (dq/dt) increases over time until it gradually reaches an equilibrium state, primarily due to the progressive reduction in the driving force (qe − qt). Furthermore, the plots presented in Figures IV.24 and IV.25 demonstrate that the adsorbate uptake, q, exhibits an upward trend with increasing initial concentration.

Table IV. 4: Kinetic models parameters for MG adsorption on HDPE/Na-MMT with different initial concentration.

C_0	q exp	Pseudo-first-order			Pseudo-second-order		
		q_e	K_1	R^2	q_e	K_2	R^2
5	0,33	0,321 ± 0,009	0,056 ± 0,006	0,971	0,380 ± 0,010	0,182 ± 0,025	0,990
20	1,37	1,315 ± 0,032	0,064 ± 0,006	0,976	1,532 ± 0,036	0,054 ± 0,006	0,992
30	1,90	1,837 ± 0,030	0,080 ± 0,006	0,986	2,085 ± 0,018	0,053 ± 0,002	0,998
50	2,30	2,191 ± 0,027	0,313 ± 0,087	0,987	2,244 ± 0,034	0,467 ± 0,211	0,991

Based on the data presented in Table IV.4, the coefficients of determination (R^2) for the pseudo-first-order values exhibit variations ranging from 0.971 to 0.987 across the four different initial concentrations of the dye. On the other hand, the R^2 coefficients for the pseudo-second-order values range from 0.990 to 0.998.

The analysis presented in Table IV.4, reveals that the coefficients of determination (R^2) associated with the pseudo-second-order model are consistently higher than those of the first-order model. Additionally, the estimated q_e values obtained from the pseudo-

second-order model demonstrate a comparable level of accuracy to those derived from the pseudo-first-order model.

These findings suggest that the pseudo-second-order model provides a better fit for describing the adsorption of MG on HDPE/Na-MMT. The superior goodness of fit and good q_e accuracy supports the pseudo-second-order model in capturing the adsorption behaviour.

GENERAL CONCLUSION

General Conclusion

The objective of this present work is to find and develop solutions to improve the structural, rheological and biodegradable properties of high-density polyethylene in order to expand its eco-friendly applications, as this material is among the most widely used and demanded polymers in the industrial field. By exploring:

- Realization of new nanocomposite films based on HDPE/clay by the technique of incorporation in the molten state;
- The influence of the montmorillonite nanoparticles geometry (MMT) on the structural and morphological properties of HDPE nanocomposites;
- Feasibility study of applying the prepared films in the field of water treatment and removal of cationic organic pollutants.

For this reason, we chose to use bentonite clay (from Maghnia, Tlemcen, Algeria) after subjecting it to purification and Na- exchange processes as an inorganic filler in nanocomposites films based on HDPE polymer. Characterizing the nanofilms with different characterization techniques. We have also applied it to an adsorption process for malachite green. The removal of malachite green dye from aqueous solution by adsorption it with HDPE/MMTs nanocomposites has been experimentally determined and the following conclusions are made:

- Optical microscopy analyzes confirmed the successful purification of natural bentonite and obtaining pure MMT particles have similar sizes, and microscope images also showed that the obtained nanocomposite films have a heterogeneous surface and morphology with good dispersion of MMT particles. The results of FTIR agreed with the results of the optical microscope, where the complete disappearance of the absorption bands at 795 and 687 cm -1 confirms the success of the purification process and obtaining MMT free from non-smectitic phases. The infrared spectra result also indicated that the polymer effectively preserved its structural integrity, due to the lower filler content, using 4% MMT by mass.
- Based on results, it can be concluded that the HDPE/MMT nanocomposites films is an interesting option for malachite green dyes removal from fresh water, it is clear that the adsorption progress has some limitations.
- The weight of the adsorbent material has a direct impact on the adsorption process. Increasing the weight of the adsorbent leads to a decrease in the quantity of dye adsorbed,

whereas the initial concentration of malachite green shows an opposite effect, with higher concentrations resulting in increased adsorption.

- By adding sodium to MMT, the nanocomposite's adsorption capacity is significantly enhanced. This addition also improves the adsorption rate and enables a higher quantity of dye to be adsorbed.
- The temperature effect on adsorption process is found to be insignificant for HDPE/Na-MMT. Thus the ambient temperature could be the best choice.
- The pH level of the solution has a significant impact on the adsorption capacity of malachite green on HDPE/Na-MMT. The best results were obtained within the pH range of 6-10.
- Among the HDPE/MMTs nanocomposites, the adsorption capacity of malachite green of HDPE/Na-MMT nanocomposite is the best, and the adsorption potential of HDPE/Treated-MMT is somewhat better than that of HDPE/bentonite. The cation exchange of mommorillonite with sodium ions increased the adhesion between montmorillonite and the matrix, resulting in good dispersion of MMT particles and obtaining intercalated nanocomposite. This addition also improves the adsorption rate and enables a higher quantity of dye to be adsorbed.
- The establishment of adsorption isotherm models revealed that the Langmuir model is the most suitable for describing the adsorption of malachite green on HDPE/Na-MMT. This model suggests a monolayer adsorption onto a homogeneous surface.
- The adsorption kinetics can be accurately predicted by employing the pseudo-second-order model.

In addition to this work, we propose the following perspectives:

- The use of high-resolution characterization tools and devices such as SEM and TEM to study the morphology of MMTS and their nanocomposites, XRD to confirm the increase of interfacial spacing of Na-MMT after cation exchange, TGA know thermal stability of nanocomposites films;
- Preparation of HDPE/MMT nanocomposites by the in-situ polymerization technique, in order to obtain an excellent dispersion of the MMT sheets in the HDPE matrix;
- Conducting further investigations on the possibility of applying HDPE/MMTs nanocomposite films in the treatment of waste water and industrial pollutants.

REFERENCES BIBLIOGRAPHY

References Bibliography

[1] Hameeda, B. H. El-Khaiary, M. I. Kinetics and equilibrium studies of malachite green adsorption on rice straw-derived char b. Journal of Hazardous Materials, 701–708, 2008.

[2] Shailesh, V. Sweety, P. Chandra, P. H. Efficient Adsorption and Photocatalytic Degradation of Malachite Green Dye Using Bentonite Natural Adsorbent. International Journal of Nanomaterials and Chemistry, 3(2);33-37, 2017.

[3] Aga, S. Etude cinétique et thermodynamique de l'adsorption de quelques colorants textiles par des résidus issus de l'industrie agroalimentaire, Universite ferhat abbas setif-1-, Memoire de Magister, 2015.

[4] Laouici,A. Boumaza, L. Contribution à l'étude de l'adsorption et la photodégradation solaire de deux colorants cationiques, Université Mohammed Seddik Ben Yahia – Jijel, Mémoire de Master, 2021.

[5] Rangabhashiyam, S. Anu, N. Selvaraj N. Sequestration of dye from textile industry wastewater using agricultural waste products as adsorbents, Journal of Environmental Chemical Engineering, 1(4);629-641, 2013.

[6] Guivarch, E. Traitement des polluants organiques en milieux aqueux par le procédé électrochimique d'oxydation avancée « Electro-Fenton ». Application à la minéralisation des colorants synthétiques, L'université de Marne-la-Vallée, Thèse de doctorat, 2004.

[7] Lemonnier, M. Viguier, M. Les textiles et leur entretien, Ed. Jacques Lanore, Paris 7e, p.104-105, 2002.

[8] Demirbas, A. Agricultural based activated carbons for the removal of dyes from aqueous solutions: a review, Journal of Hazardous Materials, 167;1-9, 2009.

[9] Douinat, O. Valorisation d'un déchet agro-alimentaire pour l'adsorption de micropolluants, Université Abdelhamid Benbadis de Mostaganem, Mémoire de Magister, 2012.

[10] Ouchene, S. Merakchi, S. Etude Cinétique et Thermodynamique de l'Adsorption d'un Colorant Organique Sur un géomatériau, Université larbi ben m'hidi (oum el bouaghi), Mémoire de Master, 2019.

[11] Bliefert, C. Perraud, R. Chimie de l'environnement : air, eau, sols, déchets, 2e éditions de boeck, Bruxelles, 2004.

[12] Rais, A. Rajeev, K. Adsorptive removal of congo red dye from aqueous solutionusing bael shell carbon, Applied surface science, 57;1628-1633, 2010.

[13] Milano, J. C. Loste, B. P. Vernet, J. L. Photooxydation du Vert de Malachite en Milieu Aqueux en Presence de Peroxyde D'Hydrogene: Cinetique et Mecanisme Photooxidation of Malachite Green in Aqueous Medium in the Presence of Hydrogen Peroxide: Kinetic and Mechanism, Environmental Technology, 16(4);329-341, 1995.

[14] Lakherwals, D. Adsorption of Heavy Metals–A Review, International Journal of Environmental Research and Development, 41-48, 2014.

[15] Saoudi, S. Hamouma, O. Adsorption d'un colorant basique bleu de méthylène sur une argile acidifié, Université A. MIRA - Bejaïa, Mémoire de Master, 2013.

[16] Abdallah, A. Bouguerra, M. Elimination du chrome hexavalent Par adsorption sur le charbon actif obtenu à partir de liège, Université de Jijel, Mémoire de Master, 2019.

[17] Koller, E. Aide-mémoire de génie chimique - 4/e édition, Dunod, Paris (France), 2013.

[18] Guignard, D. L'essentiel de la cinétique et de la thermodynamique chimique : à travers les problèmes de concours. 1992.

[19] Kuma, A. Kumar, S. Gupta, D.V. Adsorption of phenol and 4-nitrophenol on granular activated carbon in basal salt medium: Equilibrium and kinetics. Journal of Hazardous Materials, 155-166, 2007.

[20] Kacem, B. Baelhadj, A. Elimination de composés phénoliques et vert malachite par adsorption sur des billes d'alginates/ charbon actif, Université de Ghardaïa, Mémoire de Master, 2021.

[21] Bennaceur, A. Nahoui, A. Valorisation des déchets agro-alimentaire cas des pétioles de palmier (Kornaf), Université Kasdi Merbah Ouargla, Mémoire de Master Academique, 2019.

[22] Bouziane, N. Elimination du 2-mercaptobenzothiazole par voie photochimique et par adsorption sur la bentonite et le charbon actif en poudre, Universite Mentouri de Constantine, Memoire de Magister, 2007.

[23] Yahiaoui, N. Moussaoui, R. étude de l'adsorption des composes phénoliques des margine d'olive sur carbonate de calcium, hydroxyapatite et charbon actif, Université Mouloud Mammeri Tizi Ouzou, Mémoire de Magister, 2012.

[24] Ghali, S. Etude de la carbonisation d'un précurseur végétal, les noyaux d'olives: utilisation dans le traitement des eaux, Université du 20 Août 1955-Skikda, Mémoire de Magister, 2008.

[25] Aluigi, A. Rombaldoni, F. Tonetti, C. Jannoke, L. Study of methylene blue adsorption on keratin nanofbrous membranes, Journal of Hazardous Materials, 268;156–165, 2014.

[26] Sabarish, R. Unnikrishnan, G. Novel biopolymer templated hierarchical silicalite-1 as an adsorbent for the removal of rhodamine B, Journal of Molecular Liquids, 272;919–929, 2018.

[27] Temkin, M. J. Pyzhev, V. Recent modifications to Langmuir isotherms, Physiochim., URSS, 12;217-22, 1940.

[28] Boulkrah, H. Etude comparative de l'adsorption des ions plomb sur différents adsorbants, L'université du 20 Août 1955-Skikda, Mémoire de Magister, 2008.

[29] Edeline, F. L'épuration physico-chimique des eaux, théorie & technologie des réacteurs, 2 eme édition entièrement revu et complétée

[30] Suzuki, M. Adsorption engineering, New York, NY: Elsevier Science Publishing Company, 1991.

[31] Giles, C. H. Smith, D. A general treatment and classification of the solute adsorption isotherm part. II. Experimental interpretation, Journal of Colloid and Interface Science, 47;766-778, 1974.

[32] Choufa, N. Epuration des eaux usées: l' élimination des micropolluants dans les eaux usées par un matériau argileux, Université Mohammed Chérif Messaadia Souk Ahras, Memoire de Magister, 2013.

[33] Bouderbala, O. Tahar, K.M. Valorisation d'un déchet vert par Adsorption, Université Abdelhamid Ibn Badis Mostaganem, Memoire de Master Acadimique, 2021.

[34] Vi Vi, D.T. Matériaux Composites Fibres Naturelles/Polymère Biodégradables Ou Non, L'université de Grenoble, Thèse de Doctorat, 2006.

[35] Hanemann, T. Szabó, D. V. Polymer-Nanoparticle Composites: From Synthesis to Modern Applications, Journal Materials, 3;3468-3517, 2010.

[36] Stephen, G. Martin, R. T. Definition of clay and clay mineral: joint report of the AIPEA nomenclature and CMS nomenclature committees. Clays and clay minerals 43;255-256, 1995.

[37] Searle, A. B. The natural history of clay. The University Press, 1912.

[38] Velde, Bruce. Introduction to clay minerals: chemistry, origins, uses and environmental significance. London: Chapman & Hall, 1992.

[39] Kodama, H. Grim, R. E. clay mineral. Encyclopedia Britannica, 17 Aug. 2022, <https://www.britannica.com/science/clay-mineral>. Accessed 7 April 2023.

[40] Mohammad, J. Qaiss, A. Rachid, B. Nanoclay reinforced polymer composites, 2016.

[41] Neeraj, H. L. K. Mohan, C. Basics of Clay Minerals and Their Characteristic Properties. Clay and Clay Minerals, IntechOpen, 22 Dec 2021.

[42] Moore, D. M. Robert, C. Reynolds, Jr. X-ray Diffraction and the Identification and Analysis of Clay Minerals. Oxford University Press (OUP), 1989.

[43] Nabil, B. Caractérisation, valorisation des bentonites Algériennes pour l'utilisation dans l'industrie pharmaceutique et cosmétique: cas du gisement de Maghnia, Tlemcen-Algérie, 2022.

[44] Hang, P. T. Brindley, G. W. Methylene blue absorption by clay minerals, determination of surface areas and cation exchange capacities. Clays and Clay Minerals 18;203-212, 1970.

[45] Murray, Haydn, H. Structure and composition of the clay minerals and their physical and chemical properties. Developments in clay science 2, 7-31, 2006.

[46] Barton, C. D. Karathanasis, A. D. Clay minerals. Encyclopedia of soil science 10, 2002.

[47] Abeywardena, Sujani Baddrika Yapa. Application of nanoclay on polyester fabrics as a bio-inspired approach to improve moisture management. Diss. 2018.

[48] Velde, B. Composition and mineralogy of clay minerals. Origin and mineralogy of clays: clays and the environment, 8-42, 1995.

[49] Karima, N. Khaoùla, B. Hanane, D. Elaboration et Caractérisation d'un Matériau Inorganique (destiné à la Préparation des Matériaux Composites), Université Mohamed Boudiaf-M'sila, Mémoire de Master, 2021.

[50] Grim. Ralph, E Necip, G. Bentonites: geology, mineralogy, properties and uses. Elsevier, 2011.

[51] Ombaka, O. Characterization and classification of clay minerals for potential applications in Rugi Ward Kenya. African Journal of environmental science and Technology, 10(11);541-431, 2016.

[52] Murray. Haydn, H. Applied clay mineralogy: occurrences, processing and applications of kaolins, bentonites, palygorskitesepiolite, and common clays. Elsevier, 2006.

[53] Boukadah, N. Etude de l'adsorption de micropolluants organiques sur la bentonite, L'université du 20 Août 1955-Skikda, mémoire de magister, p39, 2007.

[54] Kanouri, R. Labide, A. Adsorption du phénol sur la bentonite de Maghnia, Universite Kasdi Merbah Ouargla, Mémoire de Magistère, p7, 2013.

[55] Mark, J. E. Polymer Chemistry: An Introduction. CRC Press, 2006.

[56] National Historic Chemical Landmarks. Bakelite: The World's First Synthetic Plastic http://www.acs.org/content/acs/en/education/whatischemistry/landmarks/bakelite.html American Chemical Society. Accessed 07/04/2023.

[57] Moad, G. Rizzardo E. Polymer Science. Elsevier, 2013.

[58] Frisch, H. L. (Ed.). Polymer Synthesis: Theory and Practice; Fundamentals, Methods, Experiments. Springer, 2014.

[59] George, O. Principles of Polymerization. 4th ed., Jhon Wiley & Sons, 2004.

[60] Carraher Jr, C. E. Introduction to polymer chemistry. 4th ed., CRC press, 2017.

[61] Olagoke, O. Kolapo, A. Handbook of Thermoplastics. CRC Press, 2016.

[62] Vinny, R. Sastri. Plastics in Medical Devices. 3rd ed., Science direct, 2022.

[63] William, D. C, David G. R. Materials Science and Engineering an introduction. 10th ed., Wiley, 2017.

[64] Robert, O. Polymer Science and Technology. 1st ed., CRC Press, 2000.

[65] Mariam, A. Deepalekshmi P. Marcelo, A. Polymer Science and Innovative Applications. Elsevier, 2020.

[66] Kantesh, B. Vivekn V. et al. Biosurfaces: A Materials Science and Engineering Perspective. 1st Ed., John Wiley & Sons, 2015.

[67] Ronkay, F. Molnár, B. Nagy, D. et al. Melting temperature versus crystallinity: new way for identification and analysis of multiple endotherms of polyethylene terephthalate. Journal of Polymer Research, 27;372, 2020.

[68] Anshuman, S. Introduction to Plastics Engineering. Elsevier, 2018.

[69] Kuo, Shiao-Wei, Shih-Chi Chan, and Feng-Chih Chang. Effect of hydrogen bonding strength on the microstructure and crystallization behavior of crystalline polymer blends. Macromolecules, 36(17):6653-6661, 2003.

[70] Zhaohui, T. Chaoliang, H. Huayu, T. et al. Polymeric Nanostructured Materials for Biomedical Applications, Journal of Progress in polymer science, 60;86-128, 2016.

[71] Charles, C. O. Nanocomposites: An Overview. International Journal of Engineering Research and Development, 8(11);17-23, 2013.

[72] Sati, N. Musa, R. Rahul, K. Polymeric Nanocomposites: Theory and Practice. Hanser Publishers, 2008.

[73] Ahmet, G. Introduction to Polymer–Clay Nanocomposites. Taylor and Francis Group, 2016.

[74] Galimberti, M. Cipolletti, V. R. Coombs, M. Applications of Clay–Polymer Nanocomposites. Handbook of Clay Science. Elsevier, 539–586, 2013.

[75] Manuel opératoire CP2K service laboratoire de Skikda, INTEDRA, 23 juin 2000.